DESIGN OF A NOVEL ELECTROCHEMICAL CELL FOR ELECTROCHEMICAL EXFOLIATION OF GRAPHITE INTO GRAPHENE

A Thesis
Presented to
The Academic Faculty

by

Jose A. López-Monís

In Partial Fulfillment
of the Requirements for the Degree
Master of Science in Mechanical Engineering in the
Woodruff School of Mechanical Engineering

Georgia Institute of Technology
December 2020

DESIGN OF A NOVEL ELECTROCHEMICAL CELL FOR ELECTROCHEMICAL EXFOLIATION OF GRAPHITE INTO GRAPHENE

Approved by:

Dr. Seung Woo Lee Advisor
School of Heat Transfer, Combustion and Energy Systems
Georgia Institute of Technology

Dr. Peter J. Hesketh
School of Micro and Nano Engineering
Georgia Institute of Technology

Dr. Hailong Chen
School of Micro and Nano Engineering
Georgia Institute of Technology

Date Approved: [November 30, 2020]

TABLE OF CONTENTS

LIST OF TABLES

LIST OF FIGURES

SUMMARY

Keywords: Electrochemical exfoliation, graphite, graphene, electrochemistry, nanomanufacturing, electrochemical cells.

Electrochemical exfoliation approach has recently become one of the most studied and improved graphene production methods due to several advantages, such as its simple required set-up, its environmentally friendly nature originated by the use of less hazardous chemicals, or the process' related low-costs. Even more, last years' research has allowed the user capacity to control the product thickness.

The objective of this project is to develop a cost-effective novel electrochemical cell to produce graphene from graphite. Furthermore, the general scope tries to address one of the main limitations of the electrochemical exfoliation process, which is the necessity of a monolithic graphite to successfully achieve the material exfoliation. Hence, different designs are proposed and built in order to determine whether or not they are suitable for this task.

In addition, a process parameter study is developed to understand the implications that the specific conditions have over the produced graphene. Variations in the electrolyte concentration, in the applied voltage bias and in the pre-exfoliation intercalation process duration are introduced in the different designs.

From the graphene oxide characterization carried out using X-ray photoelectron spectroscopy (XPS) and Raman spectrometry, it is concluded that the proposed processes

produce low quality multi-layer graphene oxide. Nevertheless, these novel approaches conform the basis for further research in this area.

1 INTRODUCTION

Graphene is a single atomic layer of graphite formed by sp^2 carbon atoms that lay in a honeycomb structure made of hexagons[1]. Research efforts on this material have grown since its discovery due to the exceptional properties it presents.

First, in the mechanical area, graphene has the best strength related properties of all the materials discovered. When compared to the most common structural material, steel, graphene has an ultimate strength of 130 GPa, while the structural steel has 0.4 GPa [2]. Furthermore, graphene also has extraordinary density characteristics. It weighs 0.77 mg per meter square, which means a 100 square meter area can be covered with less than 1 g of this material. Finally, these mechanical properties are complemented with elasticity. Pure graphene presents a Young's modulus of 0.5 TPa.

On the other hand, graphene also has particular electronic properties. The presence of a π electron in the third dimension might drastically increase the conductivity of this material. Research over the last decades has shown that the graphene electrons and holes have zero effective mass at the Dirac points, which are the corners of the Brillouin zone that act as the transition between the valence and conduction bands. Due to the state's zero density, it presents low conductivity. However, doping the material with either electrons or holes creates a modification that improves the conductive properties[3].

Finally, graphene also creates high expectancies in the optical industry. With its capacity of white light absorbance (larger than 2.3%), multilayer graphene has been proven to be an exceptional wavelength-insensitive saturable absorption material[4]. All these

properties make graphene the ideal material for broad applications, such as energy storage devices, conductive coatings, nanocomposites for structural devices, etc.

Although the material's exceptional properties, they are directly related with the quality of the graphene. Thus, depending on the application graphene is going to serve, different qualities and characteristics are targeted. Currently, several methods that involve mainly mechanical and chemical procedures can be used for the production of graphene. However, these approaches usually are limited by a direct complex-quality correlation, and, consequently, a yield-cost relation. Hence, the highest the quality and yield, the highest the cost.

The objective of this project is to design an electrochemical cell for the mass production of graphene focused towards a cost-effective solution. Currently, most of the setups that involve electrochemical exfoliation use as precursor material a rigid graphite material, such as a graphite rod or highly oriented pyrolytic graphite (HOPG). This last type of graphite is used to maximize both the production yield and quality. However, it also increases the price of the process. For instance, HOPG grade B, which is a medium quality category, is priced at $300 for a 5x5x1 mm plate. Hence, in order to reduce the total cost of the cycle, different electrochemical cells which use graphite powder as bulk material are designed and tested.

Furthermore, a comparison between the graphene obtained through the different proposed cells is carried out. Production yield and graphene characterization using X-ray photoelectron spectroscopy (XPS) and Raman spectrometry constitute the basis for this

section of the project. Moreover, for each designed setup, a variation of the control parameters of the process is implemented to provide a deeper understanding of the matter.

2 LITERATURE REVIEW

The 2D material graphene was first recognized in 1859, when the English Chemist Benjamin Collins Brodie discovered the layered nature of graphite oxide [5]. Afterwards, the research on this area incremented exponentially. In 1962, the first graphite flakes were isolated by Boehm et al. by using Transmission Electron Microscopy (TEM) and X-ray [6]. However, it was not until 1987 when the term "graphene" was first used. Although more progress was made in the research of these monolayer material, graphene was not obtained until 2004, when Professors Andre Geim, Konstantin Novoselov and their colleagues of the University of Manchester and the Chernogolovka's Microelectronics Technology Institute[7] used tape as an exfoliation process to separate this material from graphite.

However, 16 years after its discovery and first obtention, graphene is not extensively used in almost any industry. As explained before, theoretically, graphene presents the best properties within all the materials in several industries. But depending on the industry, different quality and characteristics graphene are needed in order to be suitable for a specific area. Therefore, the obtention process needs to vary to adapt to the requirements of each of the industries. Furthermore, the variation of the process does not only affect the result, but also the final price of the product. For instance, the crumpling of graphene in the out-of-plane direction- which could be caused by finite point defects of the structure[8]- of the monolayer plane worsens the mechanical properties of the material. Thus, the quality of the graphene does affect its properties.

2.1 Graphene production techniques

There are two types of process that are used to produce graphene:

2.1.1 Bottom – up approach

This technique consists in creating a layer by layer a material by adding building blocks of molecules. This is a significant complex process that tends to be time consuming. As an example of this method, all nature systems are built by using this bottom-up approach. For instance, the growth of a tree is given by the addition of layers of molecules and not by the reduction of a larger tree. The main advantage of this technique is that molecules are created as customer preference. This means that the producer can control the resolution or quality of the product and atomic-level accuracy can be achieved. On the other hand, this technique also presents important drawbacks. The main limiting factor is the existing technology. In order to precisely create a perfect structure of molecules to make a layer of a material, extremely high accuracy equipment is needed. Even more, if this technology is available, the building and operation costs related to this equipment do increment process price in a meaningful way. In conclusion, a bottom-up approach would result in a high-quality graphene, but this method represents an expensive and time-consuming process[9].

2.1.2 Top-down approach:

Following the previous tree example, this process could be explained as cutting a tree in order to create a wood beam. This means that from a larger body made of a material, a smaller part made of the same material or an evolution is obtained. This approach presents

several advantages. First, the user can perfectly locate the desired entity. For instance, the graphene can be directly placed in the desired location and can be also directly integrated in the electronic structures. Another improvement this operation has when compared to the bottom-up approach is the process costs. While the bottom-up approach usually can be presented as an expensive method due to the necessary high-technological equipment needed, the top-down approach does not need this type of equipment. In this type of procedure, most part of the budget is dedicated to the bulk material from where the subtraction happens. Nevertheless, it also has several drawbacks. The main one is the lack of purity. Because of the own fact of breaking down a body from its initial state to different fragments, the resulting material suffers from a quality deterioration. The rough nature of the separation method worsens the structure of the final product. Therefore, graphene obtained from a top-down approach usually can be described as a lower quality material than the graphene that results from a bottom-up approach. To summarize, a top-down procedure is a fast, cost-effective method that in general produces a non-perfect quality graphene[10].

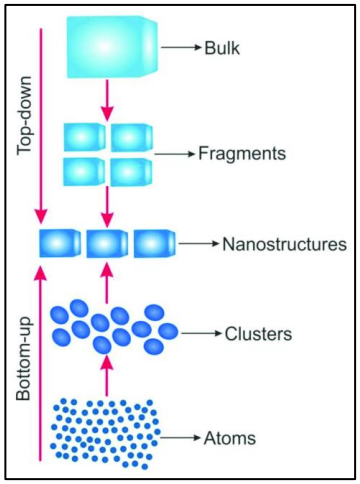

Figure 1: Bottom-Up approach vs Top-Down approach[11]

Bottom-up and top-down approaches are the global type of procedure used to obtain graphene. Now, the specific different methods of each of the approaches are presented:

2.1.3 Mechanical Exfoliation

2.1.3.1 Micromechanical exfoliation or Scotch tape approach:

This method is the one used by Professors Andre Geim and Konstantin Novoselov when they succeeded to separate the first graphene from graphite. Normally, mechanical exfoliation processes use either a shear or a normal force in order to achieve the fragmentation of a material. However, this peeling technique brings together both types of forces, which facilitates the exfoliation of graphene. As explained before, graphite is formed by multiple layers of graphene. The fact that makes this method effective is the low bending energy and friction between adjacent layers of graphene[12]. However, limitations make this approach not feasible for mass production of graphene. Every cycle of the process creates only micrometer-size pieces of multilayer graphene. As it can be inferred, the micromechanical exfoliation is part of the top-down approach because from a bulk material (graphite), the user separates layers of graphene using adhesive materials.

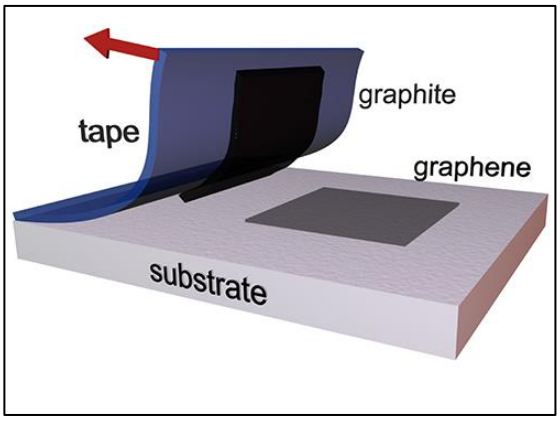

Figure 2: Micromechanical exfoliation of graphite[13]

2.1.3.2 Liquid phase exfoliation by sonication:

This mechanical exfoliation method is based in bombing ultrasonic beams against the bulk material which is immersed in a liquid-phase solvent. Hernandez et al.[14] published in 2008 an article where one of the first high-yield productions of graphene was reported. Their method used N,N–dimethylformamide (DMF) and N-methylpyrrolidone (NMP) as organic solvent. This group dispersed graphite powder in the liquid mixture mentioned above, which was followed by sonication and centrifugation. After only 4 years of the first ever obtention of graphene, an admirable 28% of monolayer graphene from all the graphene was achieved. However, the main drawback this approach has is a non-practical yield. Only a 0.01 mg/mL concentration was secured. Although these results were not appropriate for mass production, it opened a new stage of research which has increased the efficiency of this process by iterating with different parameters, such as sonication time, varying graphite concentration, changing solvent or adding polymers. However, different limitations of this technique have also been proven. The main one is the low-quality of the graphene[15,16]. This is caused by a cavitation effect due to the sonication process, which occurs in liquids where fast changes of pressure generate cavities of vapor, which collapse and produce an instant increment of temperature and pressure[17,18]. On the one hand, for the process of exfoliation, the cavitation phenomenon is beneficial because it increases the abruptness of the process. However, on the other hand, this same harshness damages the graphene by inducing more defects or oxygen groups[19].

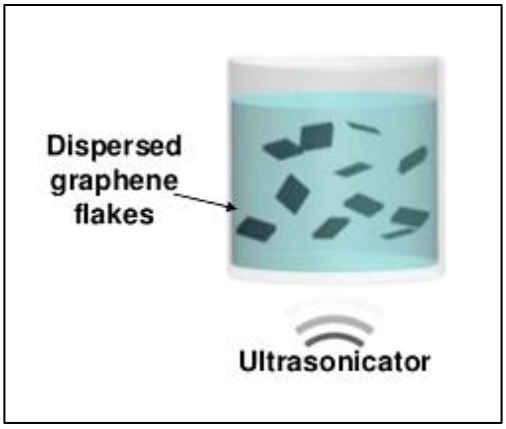

Figure 3: liquid-phase exfoliation[20]

2.1.3.3 Ball milling:

Here, shear force is the main instrument to generate the exfoliation. It consists in introducing into a chamber both metal spheres and graphite flakes and, afterwards, rotating or agitating it so that all the bodies inside collide against each other. As exhibited in Figure 4, two main phenomena occur during this process. First, balls roll over the graphite flakes, inducing a shear force over them that leads to exfoliation. Second, a vertical collision between sphere and graphite bodies which produces the fragmentation[21]. Consequently, type 1 way is desired in order to obtain large-size graphene flakes. However, the second type of collisions cleaves the graphite, reducing thus the size of graphene, and, even more, it modifies the hexagonal structure of graphene by transforming it into an amorphous and non-equilibrated crystal.

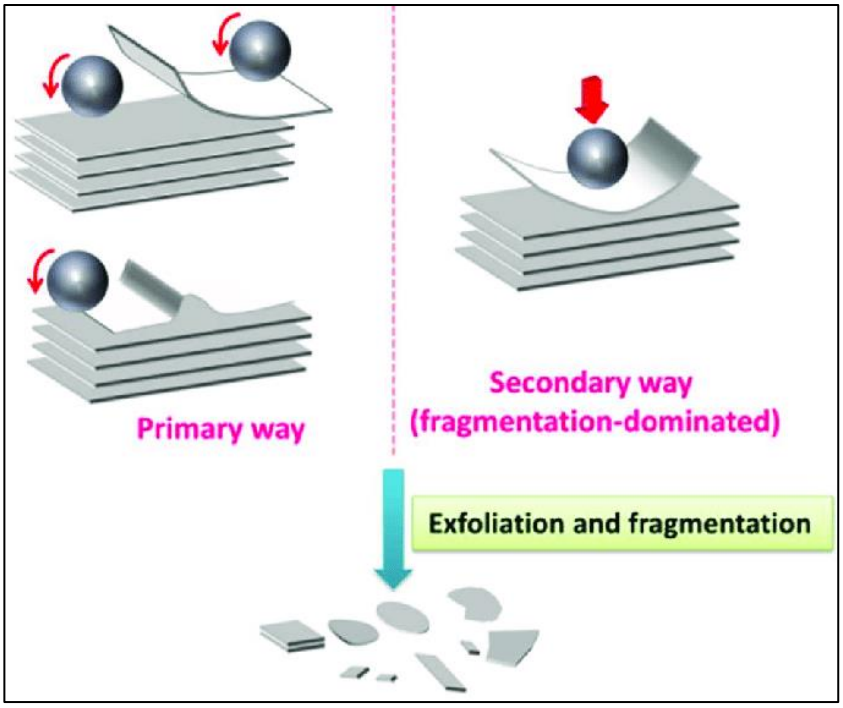

Figure 4: Ball milling exfoliation[21]

2.1.4 Chemical Vapor Deposition (CVD)

This process consists in the interaction and reaction between a substrate and a volatile environment, which results in a thin layer of the desired product over the substrate surface[22]. Typically, the process is given in a reaction chamber where certain conditions are set, such as a high temperature or pressure. Also, the speed of the reaction and the deposition tend to be slow, so that only micrometers of thickness are achieved per hour. However, as this process is a bottom-up type of process, its main advantage is the quality of the product. On the other hand, as a high temperature and toxic gases for the chamber reaction are often needed, CVD demands a quite high energy to proceed, increasing thus the cost and the environmental impact of the cycle. In terms of graphene, CVD is divided in two steps. First, a pyrolysis of a material to create a layer of carbon and, second, the modification of the carbon structure to achieve the desired graphene. Both steps need

impressive amounts of heat (over 2500 °C), so metal catalysts are used. Although the introduction of these catalysts, the heat the process needs is still considerable (around 1000 °C). Usually, Methane (CH_4) is used to provide the carbon molecules, and copper is used as the substrate, where the graphene layers deposit[23]. Boyd et al.[24] developed an improvement of the CVD approach, the plasma-enhanced CVD (PECVD), in which the necessary energy is lower than in the traditional method, and the production results in a higher quality graphene. The setup is based on the typical CVD process, where copper is used as substrate. However, the California Institute of Technology's research team added cyano radicals, which etch copper at 20 °C (68 °F)[25], to a hydrogen-methane plasma. Given this plasma environment, the etch and growth processes occur faster than in traditional CVD without the need of high temperatures (<420°C) and with a few-defect graphene as result.

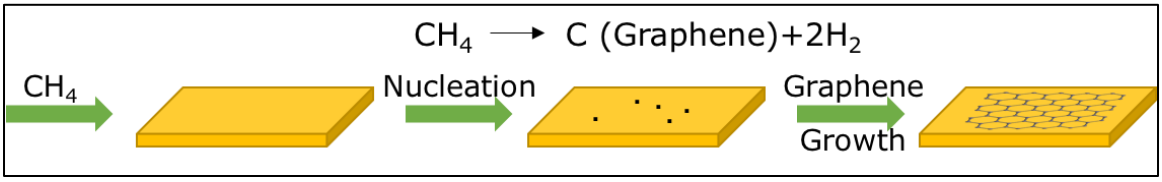

Figure 5: CVD of graphene[26]

2.1.5 Chemical Exfoliation

Again, this method has 2 main steps: increase the interlayer spacing by lowering the Van der Waals forces between the layers and, afterwards, separate the 2D layers by applying a gradient of temperature or sonicating the sample. This approach is based on the Hummer's method[27], which describes a procedure to obtain graphitic oxide using an anhydrous mixture of sodium nitrate, sulfuric acid and potassium permanganate. For

graphite exfoliation, strong oxidizing agents like sulfuric acid, phosphoric acid or potassium permanganate must be used. Afterwards, two available options depending on the desired graphene can be chosen. If a monolayer product is needed, sonication in a solution of DMF (N, N - dimethylformamide) is carried out. The other available option is to produce a multilayer graphene, which can be obtained by density gradient ultracentrifugation[28,29]. However, due to the high oxidation power required by the graphite to exfoliate, the percentage of oxygen groups in graphene exceeds the limit of adequate properties. Also, this oxidation process may severely damage the honeycomb lattices of graphene, so a high temperature step must be added afterwards to recover the initial structure[30]. Therefore, a reduction step must be added at the end of the Hummer's process For instance, hydrazine monohydrate[31] could be used as reduction agent.

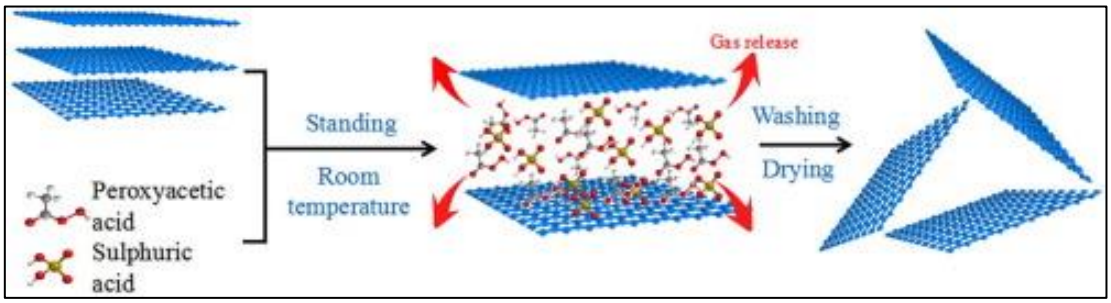

Figure 6: Chemical exfoliation of graphite[32]

2.1.6 Electrochemical exfoliation

This method is part of the family of wet chemical exfoliation approaches based on Hummer's method[27]. However, instead of using harsh oxidant agents, it takes advantage of the electric conductive properties of the material that is desired to exfoliate. Typically, the electrochemical exfoliation cell is formed by a power supply that brings the voltage, a working electrode (graphite body), a counter electrode (Platinum) and the electrolyte. The

compound which needs to be exfoliated works as one of the electrodes of the configuration, attracting thus opposite charged ions that intercalate within the layers of the material, which forces the exfoliation. This approach presents several advantages when compared to other graphene obtentions procedures. First, as a top-down process, the related costs are lower than in the molecular assembly methods, such as Chemical Vapor Deposition. Second, as the exfoliation is carried out by the electrical ion intercalation, harsh oxidants are no longer compulsory, so other electrolytes such as inorganic salts may be used. Furthermore, the absence of these agents improves the quality of the resulting graphene, reducing the percentage of defects and oxygen groups in the material. Moreover, the modification of the parameters of the approach allow the variation of presence of oxygen groups depending on the desired application of the graphene[33]. Deeper studies of this matter have revealed that a one-step obtention of graphene process and its consequent direct application in the industry may be achieved. For instance, this product is adequate to the energy storage, electronics, or nanocomposites industries. However, the main limitation of this approach is the necessity of a continuous body that brings the voltage to the graphite. Generally, a graphite foil or rod or a highly oriented pyrolytic graphite (HOPG) body are used as electrode. In the ideal case, the electrolyte's ions intercalate in the exterior surface of the material, exfoliating then the exterior graphene monolayer and allowing thus the intercalation in the next layer. However, the exfoliation happens simultaneously in all the graphite, which reduces the efficiency of the process. These multiple intercalations cause the separation of multi-layer graphene. Furthermore, the highest the desired production, the higher the area of contact between electrolyte and graphite material. Hence, electrochemical exfoliation efficiency may be reduced while the production increases[34].

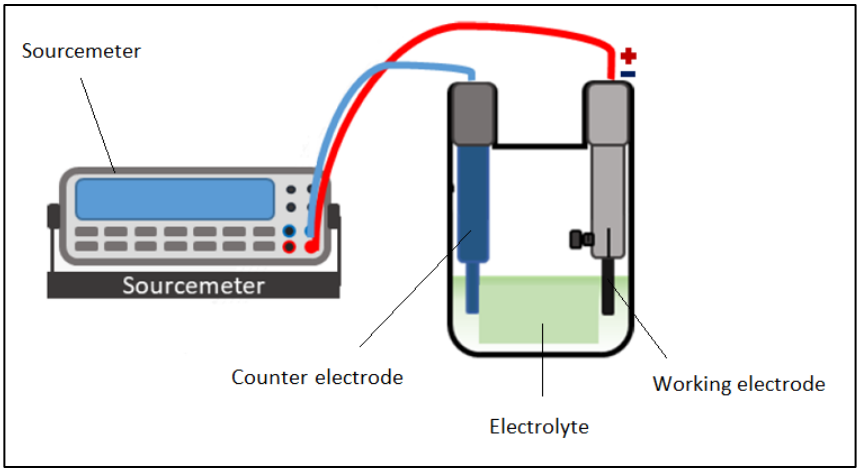

Figure 7: Electrochemical exfoliation approach

Although the set-up shown in Figure 7 is mainly used, some research groups have developed working alternatives. Liu et al.[35] designed a novel configuration where two pencil cores acted as both working and counter electrode, as Figure 8 illustrates. Here, the voltage alternates between a positive and a negative value after a constant period of time. Hence, a repetitive exfoliation of both electrodes is given, increasing thus not only the efficiency but the amount of graphene produced in one set-up. This modification has brought a green, cost-effective, and simple vision to the electrochemical exfoliation approach.

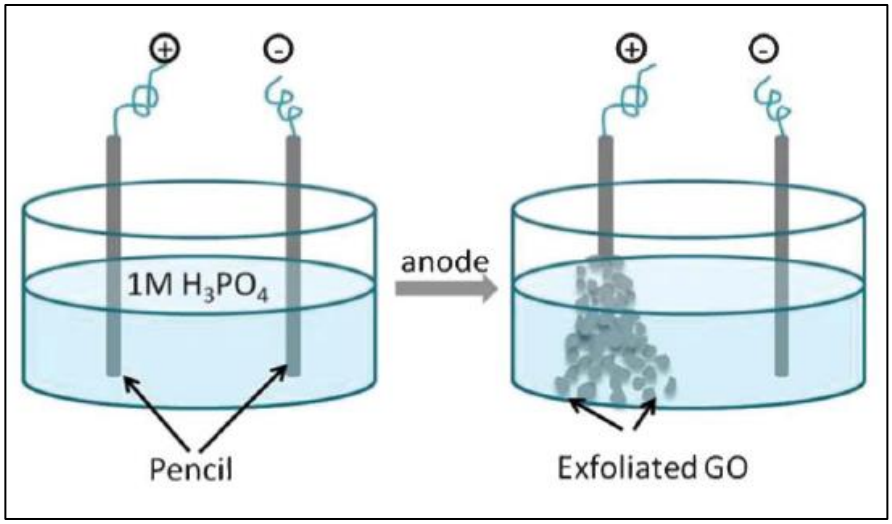

Figure 8: Alternative electrochemical configuration[35]

Although the electrochemical exfoliation process has been studied for almost a decade, most of the research groups have focused on a batch or discrete process, where once the graphite has completely exfoliated, a new set-up needs to be reassembled. Abdelkader et al.[36] designed a continuous electrochemical cell set-up that is illustrated in Figure 9. Here, the graphite is slowly introduced through the bottom of the chamber as the cathode while an electrolyte stream is introduced by a feeder on the left hand side. Exfoliation occurs and the resulting graphene flakes float and are collated by a right-hand side pipe. At the same time, those partially exfoliated flakes are deposited at the bottom of the cell and the exfoliation continues. This set-up can produce high-quality graphene without the need of a posterior sonication cycle with a rate of 0.5-2 g per hour.

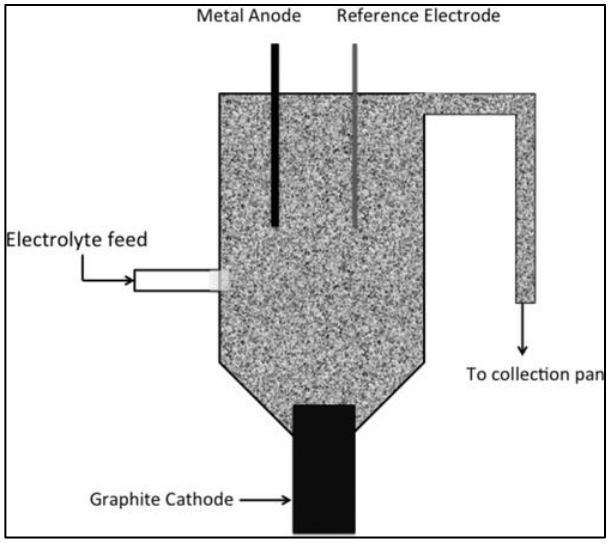

Figure 9: Cathodic continuous electrochemical cell set-up[36]

Also, Achee et al.[37] attempted to propose a continuous electrochemical exfoliation cell set-up, where flakes of graphite are inserted into the reactor and the electrolyte flows through a mesh where the material is stored. The exfoliation rate directly depends on the flow rate of graphite flakes and the area of contact between the bulk material and the electrolyte. In addition, graphite flakes need to be compressed to ensure electrical contact. Therefore, this flow of graphite flakes can be substituted by a solid and continuous graphite rod. Figure 10 shows the proposed cell.

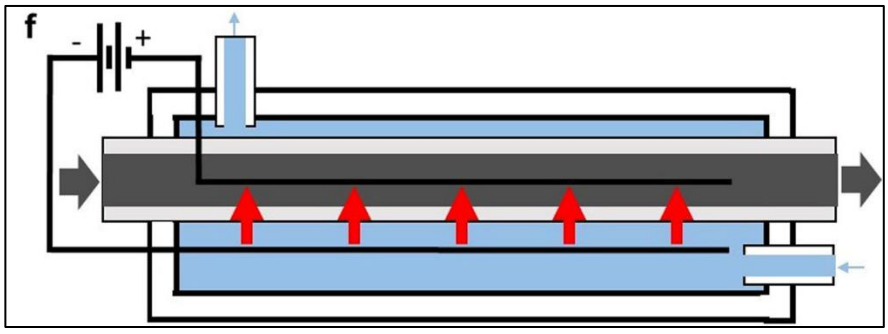

Figure 10: Anodic continues electrochemical cell[37]

Nevertheless, the electrochemical exfoliation approach faces one main limitation: the working electrode must be a monolithic graphite to ensure the electric connectivity between all the material. Hence, as explained before, this method results inefficient due to the separation of graphite flakes from the main body, which, consequently, ends in the non-exfoliation of large graphite flakes.

Liu et al.[38] tried to address this limitation by lowering the graphite rod position to the bottom. Hence, the graphene oxide was expected to float, while the graphite particles would stay in electrical contact with the main body due to gravity. Nevertheless, the yield did not improve as expected because gravity force was not sufficient to ensure this contact.

Recently, Achee et al.[37] achieved to overcome this disadvantage by designing a set-up in which graphite flakes can be exfoliated. Here, a permeable container filled with these flakes form the working electrode. In addition, a platinum wire is introduced to bring the electrical connectivity. Finally, to ensure the compression, a top movable clip closes the superior aperture of the permeable container as illustrated in Figure 11. On the other side, a graphite foil works as counter electrode. The electrochemical process happens under 0.1 M ammonium sulfate ($(NH_4)_2SO_4$) electrolyte and +10 V on the working electrode. The constant compression of the graphite flakes allows the hydroxyl ions (OH^-) to oxidize the grain boundaries of the material, consequently letting the intercalation of sulfate ions (SO_4^{2-}). Finally, gases from the reduction and oxidation process separate the layer of graphite, obtaining thus the graphene.

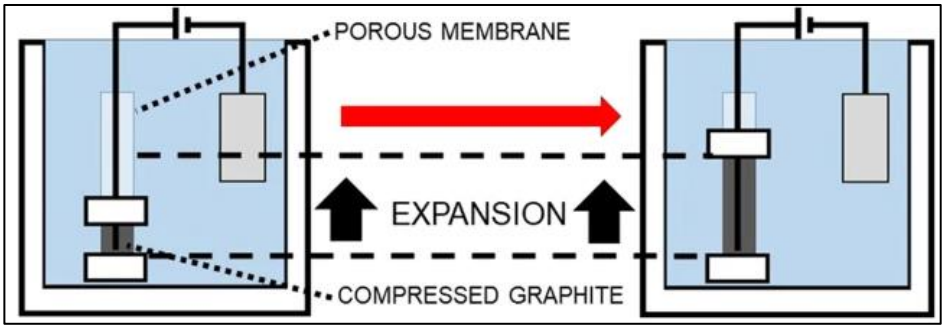

Figure 11: Electrochemical cell for the exfoliation of graphite flakes[37]

Electrochemical exfoliation approach can be divided into the following types:

2.1.6.1 Anodic electrochemical exfoliation

The graphite electrode is connected to the positive pole of the applied voltage, being therefore the anode. Hence, a positive current drives electrons out of graphite, establishing a positive charge, which attracts negative ions or anions to the material and any other co-intercalating molecule. These negative ions intercalate within the graphite layers, increasing thus the interlayer separation and facilitate the exfoliation of graphene.

2.1.6.2 Cathodic electrochemical exfoliation

The graphite material is connected in this case to the negative anode, gaining thus positively charged ions and co-intercalated molecules. This time, the cations are responsible for the intercalation and posterior exfoliation of the material.

2.1.6.3 Bipolar electrochemical exfoliation

This approach overcomes the main limitation of the cathodic and anodic electrochemical exfoliation, the need of electrical contact with graphite for the ion's intercalation. Here, an electrolyte that contains a conducting material, graphite in this case,

is polarized by creating an electric field due to two feeder electrodes. This set-up drives an electrochemical reduction and oxidation in the substrate in which the poles are induced, as Figure 12 shows.

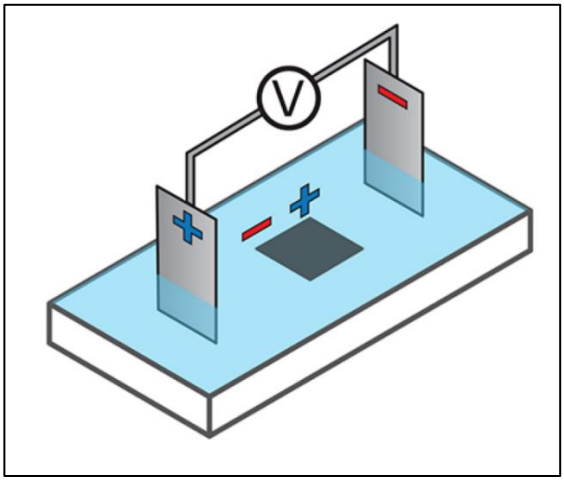

Figure 12: Bipolar electrochemical exfoliation approach[39]

In 2017, Bjerglund et al.[39] proved that bipolar electrochemistry could be applied as a viable approach towards the production of graphene. Here, a constant current is established between the feeder electrodes. A cell similar to the one shown in Figure 12 was implemented in order to exfoliate a squared 1 cm graphite foil using tetrabutylammonium tetrafluoroborate (Bu_4NBF_4) in N-methyl-2-pyrrolidone (NMP). The product characterization showed a cathodic induced exfoliation caused by the intercalation of the Bu_4N^+ into the feeder anode closest foil edge. Theoretically, by applying a voltage of 50 V between the feeder electrodes, 14.3 V can be induced in the bipolar electrodes (graphite foil). However, as the graphite exfoliates, it decreases its lateral size, so for the complete exfoliation of the bulk material, extremely high voltages are needed as Equation (1) shows. For instance, this setup would require a minimum voltage of around 1KV[39].

$$\Delta V = \frac{\Delta E \; x \; l}{L} \quad (1)$$

Where ΔV is the voltage between the edges of the foil, ΔE is the voltage between the feeder electrodes, l is the distance between edges of the film, and L is the distance between the feeder electrodes.

Two years later, in 2019, Hashimoto et al.[40] improved the bipolar electrochemical approach by substituting the previous electrolyte by a diluted sulfuric acid (H_2SO_4) one. First, in order to maximize the yield, an electrolyte concentration study was carried out. Results showed that the maximum exfoliation was obtained under a 20 mmol dm^{-3} concentration, and, at the same time, the minimum peak voltage occurred. This approach induced a theoretical voltage of 2.5 V for an square 1 mm side graphite foil, and the maximum reached voltage was 250 V. In addition, this design was proved to exfoliate graphite powders too, although a specific clarification was not stated.

2.1.7 Other alternatives

Although the rest of the approaches presented are the main methods for the production of graphene, last years' research has opened new possibilities that are being currently used or will be used in the future:

2.1.7.1 Detonation technique:

This method was discovered by Sorensen et al.[41] when they used a detonation set-up following the 'spud gun' approach. Here, a PVC pipe is filled with hair spray and with

a potato. A spark plug then ignites and the explosion leads to a potato projectile. Although the objective of this experiment was to obtain a carbon soot aerosol for water treatment, Sorensen et al. [41] found a potential mass-production of graphene technique. Instead of using hair spray, the chamber was filled with one or more carbon and hydrocarbon compounds and with one or more oxidizing agents. For instance, a mixture of acetylene or ethylene gas with oxygen can be used in the chamber. The Kansas organization claims that single, double, or triple layer graphene with a particle size between 35 and 250 nm is obtained using their method.

2.1.7.2 Soybean oil method:

Seo et al.[42] developed a variation of the CVD process where high pressure or temperature conditions are not needed. This ambient-air synthesis occurs when a nickel substrate reacts with soybean oil, a natural renewable precursor, and graphene films are deposited over the substrate.

3 DESIGN PROCESS

In this chapter the electrochemical cell designing process is presented. Firstly, different theoretical set-ups and their respective justifications are discussed. Afterward, the production conditions are stipulated, and, finally, the actual designs which have been built and tested are shown.

3.1 Proposed designs

As stated before, the main limitation for an electrochemical process is the necessity of having a monolithic material to ensure a full electrical contact. Therefore, in order to implement this approach for powder exfoliation, a method to compress the powder must be added to the design. A trivial solution to solve this issue is using gravity. In theory, gravity pushes the graphite flakes to the bottom of a recipient. This approach was tested by Liu et al.[38], but the results were not satisfactory. Hence, the gravity force was proved not to be enough. Therefore, new alternatives that address the compression issues need to be studied.

3.1.1 Centrifugation-assisted design

One possibility to address the compression challenge is to introduce rotation to the container. When an object is rotating around a fixed axis, an apparent force called centrifugal force acts on the mass, pushing it in the perpendicular outer direction of the object's trajectory. In fact, if this object wants to maintain the established trajectory, it must provide a force which is the negative centrifugal force, or centripetal force.

For the graphite exfoliation case, the graphite flakes need to be stacked against a solid part that applies the centripetal force. In this case, the walls function as this component. There are two possibilities regarding the shape of the container.

3.1.1.1 Cylindrical centrifugation-assisted design

Here, the container rotates around a centered axis. This causes all the particles, including both electrolyte and graphite flakes,r to suffer and outer force which compresses them against the wall. Figure 13 shows the 3D model of the proposed design.

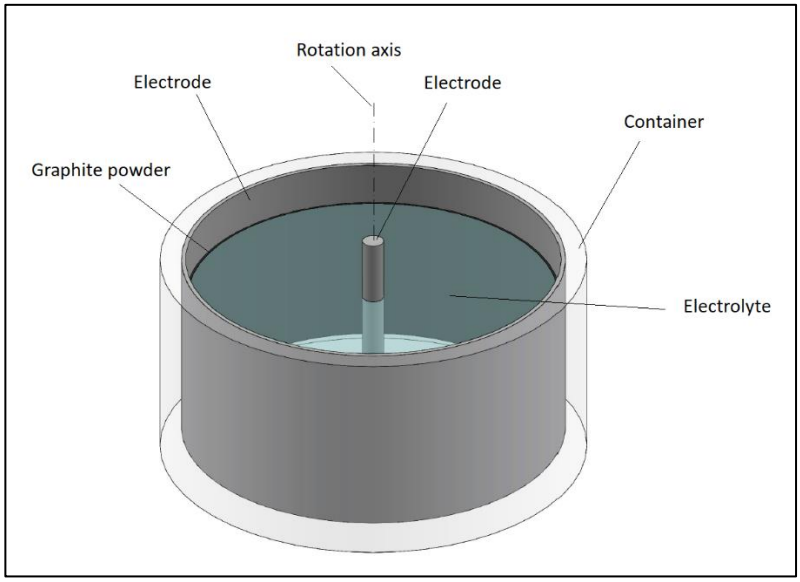

Figure 13: Cylindrical centrifugation-assisted design

This approach is ideal for large productions because the graphite flakes have a larger area to cover. However, this also represents a limitation because if the material amount is not enough, it will disperse around this area, and no contact will be given. For instance, the necessary area that graphite needs to cover is shown in Equation 2.

$$A = \pi D h \tag{2}$$

Where A is the Area covered by graphite, D is the interior diameter of the exterior electrode, and h is the height of electrode under the electrolyte. Furthermore, considering that graphite powder has a density of 1.8 mg per mm^3 [43] and an average thickness of 75 µm [44], the approximate minimum graphite powder weight can be calculated

$$A_g = \rho * T = 1.8 \frac{mg}{mm^3} * \ 0.075\ mm = 0.135 \frac{mg}{mm^2} \tag{3}$$

Where A_g is the area occupied by graphite, ρ is the graphite density and, T, the thickness of the powder. Finally, the mass of graphite should be larger than:

$$m_g \geq \ A_g * A \tag{4}$$

$$m_g \geq \ 0.135 * \ \pi D h\ mg \tag{5}$$

Figure 14 represents the behavior of both electrolyte and graphite during rotations. As it can be inferred from the illustration, graphite occupies the whole interior area of the recipient which is below the electrolyte. The superficial V shape is caused due rotation, and its slope is directly related with the speed of rotation. Hence, the highest the speed, the highest the area where graphite can deposit, and the higher the available production rate. However, electrolyte must always be in contact with the center electrode in order to have

electrical contact between anode and cathode. Also, the volume of electrolyte should not surpass a limit, or it will overflow. These issues can be solved by implementing a top cover on the vessel, but it should not be fully sealed to let the process' gasses flow to the environment.

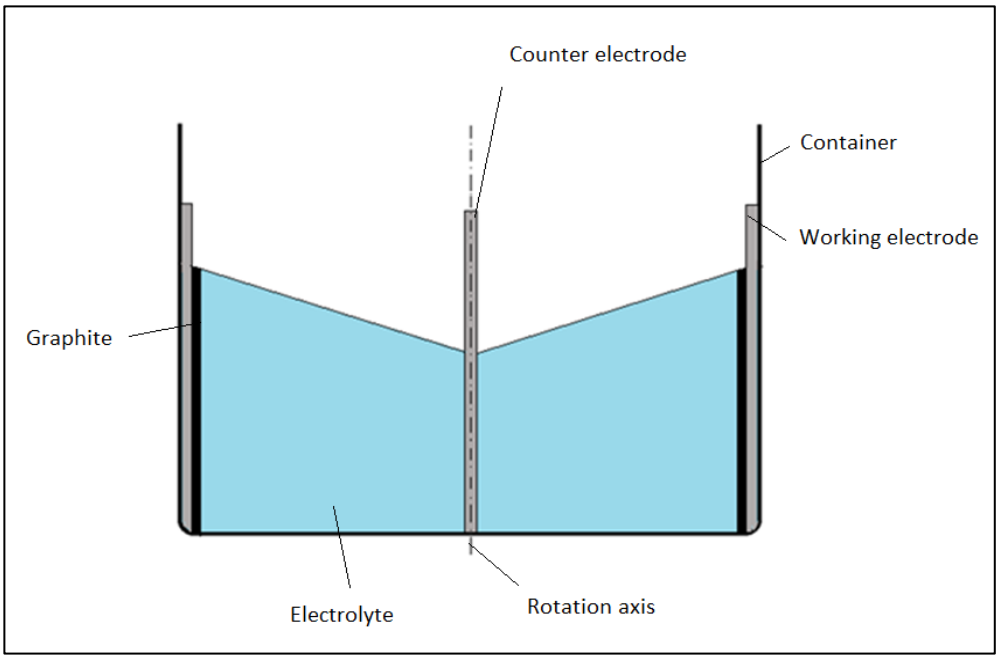

Figure 14: Cylindrical centrifugation-assisted design cut illustration

This cell also presents main limitations when compared to other cells. First, it is difficult to connect both electrodes to the DC supplier due to rotation. Second, centrifugal force depends on the speed of rotation, so successful compression rates may be only achieved at high speeds, incrementing thus the necessary process energy. Furthermore, if the configuration is not perfectly symmetrical, the set's moment of inertia would generate vibrations that would eventually damage the centrifugation machine. Third, and finally, the amount of needed electrode exponentially increases when compared to other set-ups. This electrically conductive material is necessary in order to bring the voltage to the graphite.

Hence, it must cover all the cylindrical wall. However, if the cell presents good results, the cost of fully covering the vessel with the electrode is easily recovered.

3.1.1.2 Rectangular centrifugation-assisted design

On the other hand, the rectangular centrifugation-assisted design shown in Figure 15 is more suitable for smaller productions. Here, the graphite powder is compressed against the smallest wall, so an electrode should be placed there to provide electrical contact. Thus, in order to increase the product amount, a larger smallest wall should be introduced.

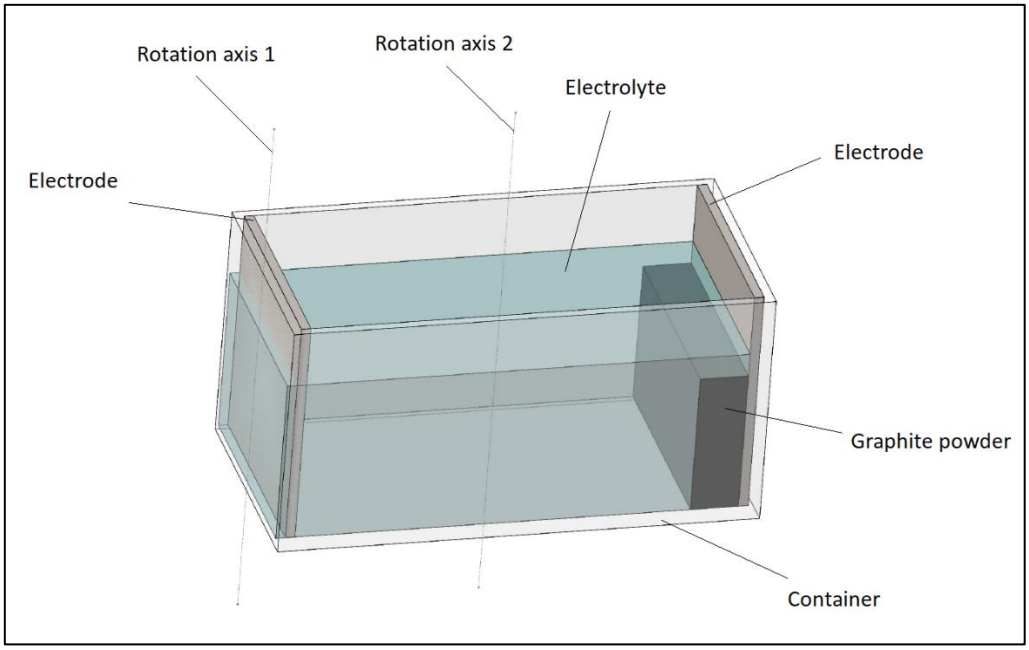

Figure 15: Rectangular centrifugation-assisted design

If the cell is inspected, there are two possible rotation axes. One is located in the center of the container, where the centroid of the recipient is located, and, the other one, is the geometrical centroid of the wall which is opposed to the wall where the graphite is stacked. Both available solutions present advantages and limitations.

The axis of rotation 1, as marked in Figure 15, has the advantage of ensuring that all the graphite power flows against the opposite electrode. Therefore, a complete exfoliation may eventually be achieved. However, the moment of inertia is not aligned with the axis, so rotation is not equilibrated, and, therefore, the centrifugal supplier needs to be designed to absorb this force.

On the other hand, the rotation axis 2 presents the advantage of being an equilibrated system with regard to inertial moments. Although the presence of graphite in theory destabilizes this equilibrium, this difference is negligible as this set-up is designed for low production rates. Nevertheless, the chances of limiting the maximum yield increase because part of the raw material could be pushed towards the counter electrode instead of the working electrode.

In terms of cost-efficiency, the initial layout of this alternative is lower than the centered design due to smaller electrodes. Nevertheless, if the material selected for electrodes is stable, these do not wear down. Therefore, they can be repeatedly used for the electrochemical exfoliation process, so the cost related to this material should not be used to choose between alternatives. The price of the electrodes is not significant when several production cycles are carried out because the higher the number of cycles, the lower the price per cycle.

3.1.2 Centered design

Here, the compression of graphite is achieved using a superior load. The design is made of a cylinder which is located in the center of the circular container. This body is

formed by a dialysis tubing which is filled with graphite powder. In addition, a load is positioned on top of the material, which brings both the compression and the necessary stiffness to the cylindrical structure. This shape conforms the working electrode, so a conductive material is needed to provide the voltage. For instance, a platinum wire could be immersed in the powder to complete this task. Finally, the counter electrode covers the walls of the container.

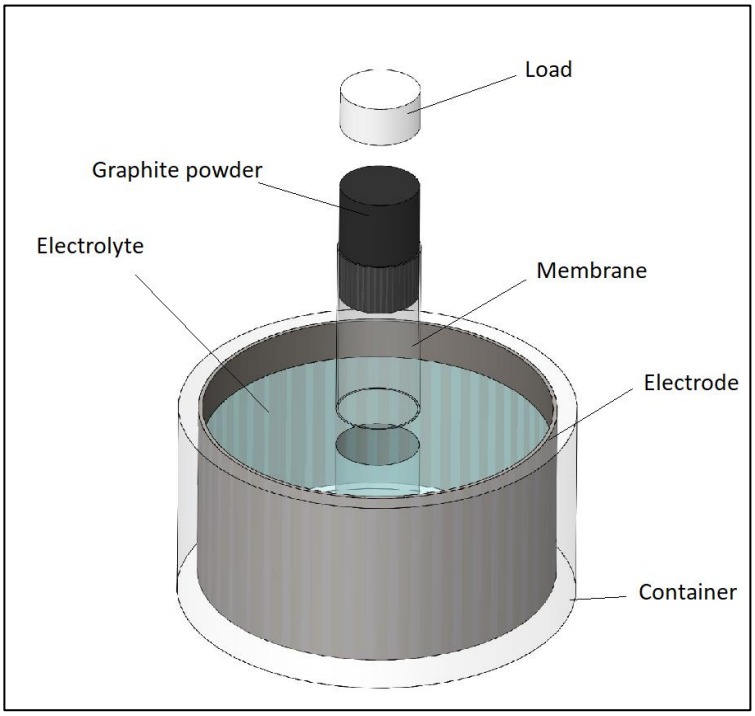

Figure 16: Centered design

Once again, the limitation of this set-up is the presence of a big area material that works as a counter electrode, which elevates the model price. Also, the pressure generated by the load may difficult the expansion of the graphite that is given during the exfoliation. This fact may produce an excessive oxidation of the material and may not allow the exfoliation. Therefore, a further study of the effects on graphite of the load's weight is

needed. Nevertheless, this electrochemical cell also presents advantages. For instance, the energy consumption of the process is minimized because the rotation is removed. Also, because of the static forces instead of the dynamic forces, this is a simple model and further structural analysis is not needed. Finally, the fact that the produced graphene is located inside the membrane facilitates the recollection step. Figure 17 illustrates a half-cut illustration of the final configuration for the centered design.

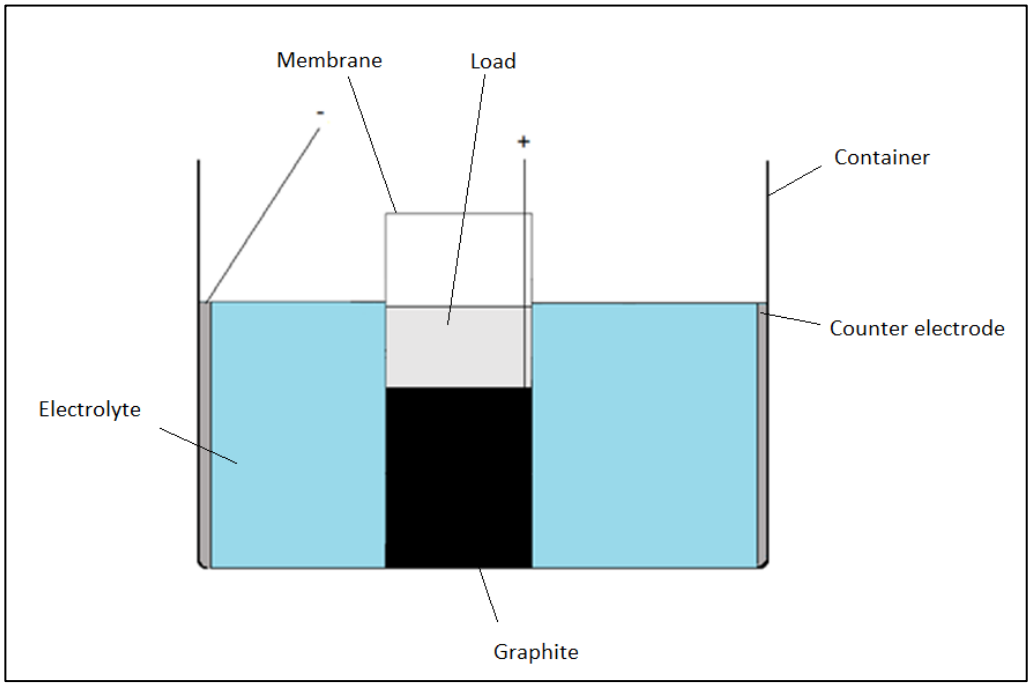

Figure 17: Centered design cut illustration

3.1.3 Bipolar anodic exfoliation

As presented in section 3.1.3, bipolar anodic exfoliation consists in inducing a voltage in the material which is going to be exfoliated. In order to complete this task, two feeder electrodes provide a constant current to the cell, which creates an induced anode and cathode in the intermediate material, being the anode the closer edge to the negative feeder electrode, and the induced cathode, the closer edge to the feeder anode[39,40]. Figure 18 shows

the 3D model of the proposed bipolar design to exfoliate graphite powder. Here, a cylindrical permeable mesh is filled with two feeder electrodes, two separators, and the graphite powder. On the top of the configuration, a load provides the necessary compression to the graphite powder. The two plastic separators act to separate the feeder electrodes and the graphite powder, so the perfect fit between them and the membrane is needed in order to not have leaks of powder towards the electrodes, which could cause a shortcut, risking then the correct performance of the set-up.

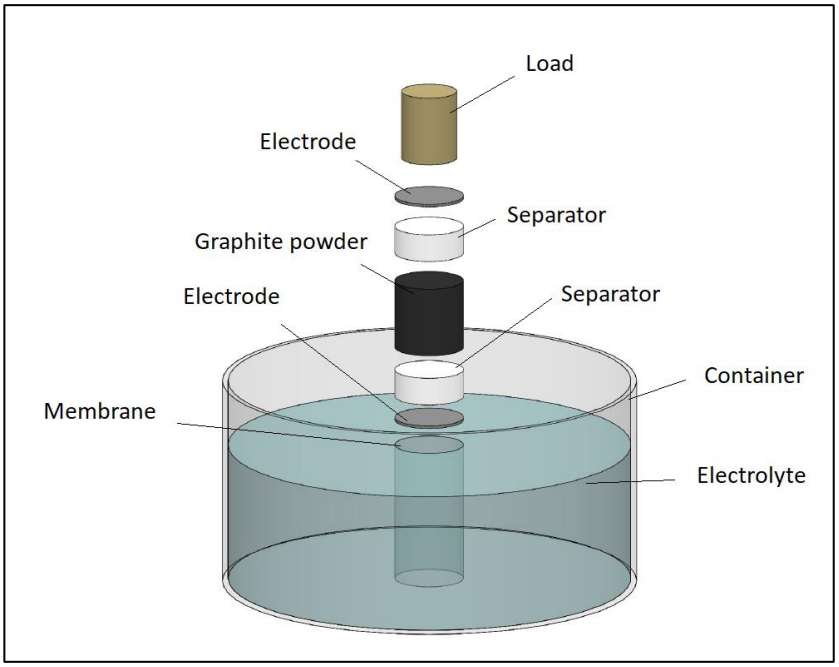

Figure 18: Bipolar anodic exfoliation

This method has already been proved to achieve graphite powder exfoliation[39], whereas other approaches have failed to do so. Nonetheless, it also has main limitations that increases the difficulty of testing it. In order to induce enough voltage in the bulk material, a high current is needed. Consequently, as the configuration resistance (electrolyte) is high, the voltage demanded from the supplier is also elevated. For instance,

Bjerglund et al. consumed more than 1000 V[40]. Furthermore, the improved design of Hashimoto et al. reduced this maximum value to about 250 V[40]. Figure 19 illustrates a half-cut of the bipolar exfoliation configuration.

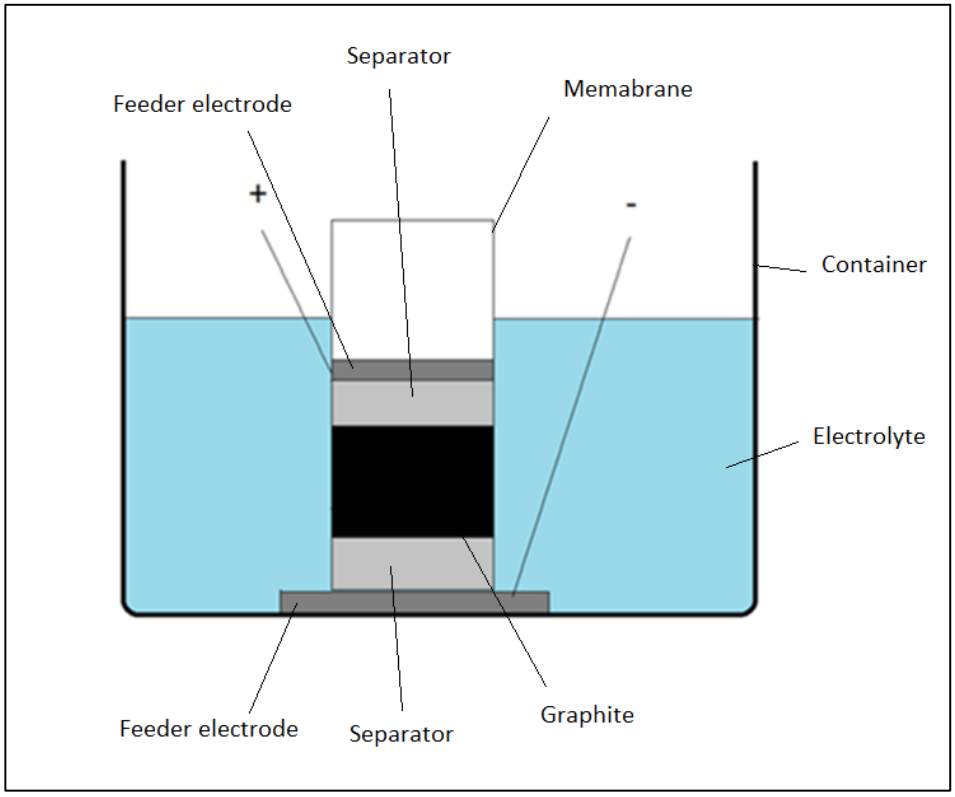

Figure 19: Bipolar anodic exfoliation cut illustration

3.1.4 Cylinder type design

Anodic electrochemical exfoliation of graphite is the most expanded and researched type of electrochemical exfoliation used to produce graphene. However, as described before, the improvements are mainly given in the exfoliation of monolithic graphite. Pre-treatment and post-treatment steps have been researched to increase both the yield and the quality of the product. Nonetheless, only a few groups have been able to provide a reliable process to exfoliate non-monolithic bodies. For instance, Achee et al.[37] developed a process

to exfoliate graphite flakes that achieved yields of around 35% (Section 2.1.6). Moreover, further improvements on the design increase their achieved yield up to 65% by adding an HNO_3 pretreatment step and modifications on the working electrode (graphite powder), such as increasing the contact surface between electrolyte and the flakes.

Here, an alternative anodic electrochemical exfoliation process is presented.

3.1.4.1 Basic idea

First, the basic idea of the cell consists of a cylinder type of structure where the feeder electrodes are two metal parts that act as the bottom and top covers. Between them, the graphite powder fills the cylinder by adapting its shape to the container's one. Finally, a top load compresses the model to ensure the electrical connection between the flakes.

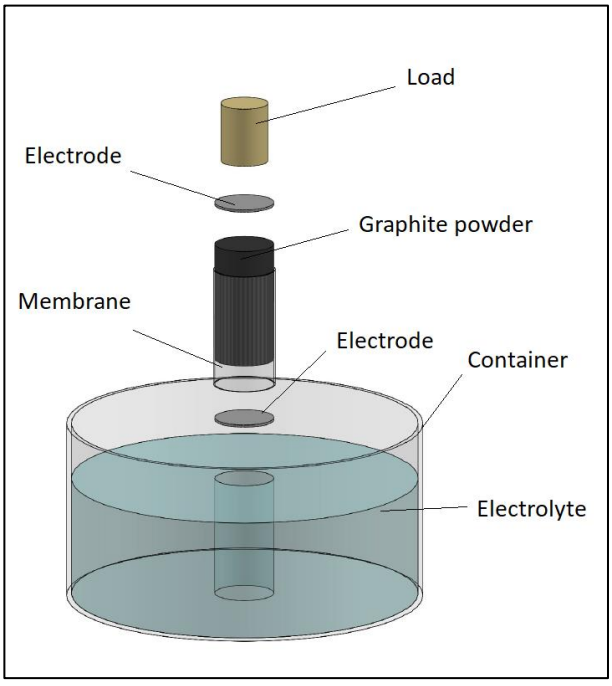

Figure 20: Anodic electrochemical exfoliation basic idea

Further developments of the basic idea are presented below.

3.1.4.2 Separator introduction

The design showed in section 3.1.4.1 cannot be implemented because, as graphite is conductive, both electrodes are electrically connected. This creates a shortcut when a voltage is applied between the feeder electrodes and, therefore, the fundamentals of the electrochemistry do not apply here.

Hence, in order to isolate anode and cathode, a non-conductive material is required. Figure 21 displays the 3D model of this cell. As it can be inferred, this body is located between an electrode and the graphite powder. The other electrode, which is in contact with the graphite, provides the electrical connection between the DC supplier and the flakes, which is essential for the success of the electrochemical process. As this approach is intended to be an anodic method, the plastic material that acts as thes separator interferes between the lower electrode, the cathode, and the working anode, built by the graphite and the upper electrode.

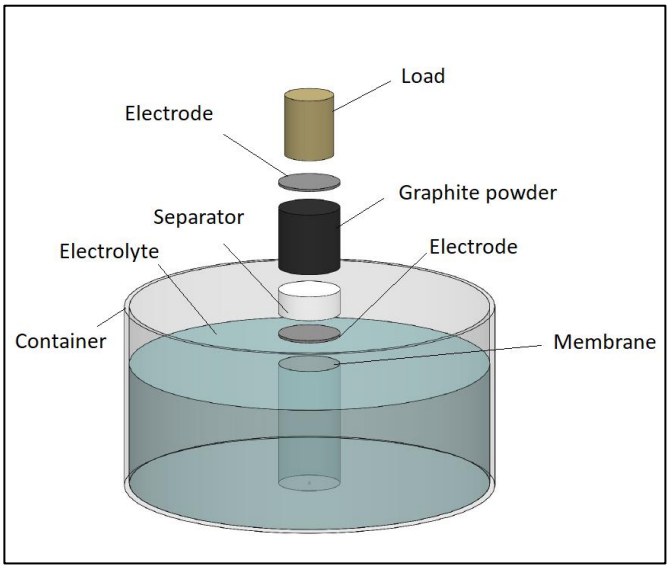

Figure 21: Anodic electrochemical exfoliation design with separator

3.1.4.3 Inside cylinder introduction

The final improvement is oriented towards mass production of graphene. The idea consists in the introduction of an inner cylinder where more electrolyte is placed. This suggestion tries to address the main limitation that is described by Achee et al.[37]. This is the lack of ion diffusion through the working electrode. Hence, a process' yield is reduced when the ions need to travel higher distances, which, in a cylindrical structure, happens when its radius increases. One possible alternative was the one introduced by this research team. They proposed reducing the radius and increasing the height of the cylinder in order to minimize the distance between the electrolyte's ions and the inner powder. However, in order to apply this solution, more electrolyte is required because a higher vessel is needed.

This project's proposal overcomes this limitation by introducing an inner cylinder which increases the surface of contact between the electrolyte and the graphite. As Figure 22 shows, the contact surface between the electrolyte and the graphite powder is now:

$$A_c = (D + d)\pi H \tag{6}$$

Where D is the diameter of the external cylinder, d is the diameter of the internal cylinder, and H is the height of the body formed by the graphite powder.

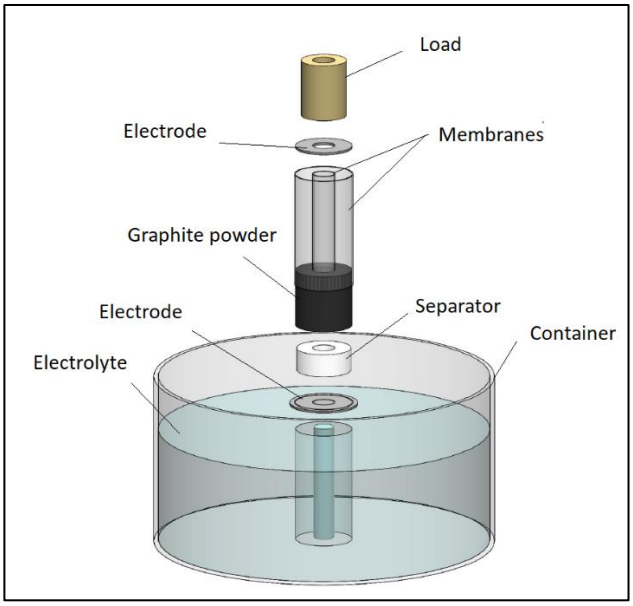

Figure 22: Anodic electrochemical exfoliation design with interior membrane

The advantages of this electrochemical cell are the simplicity of the model, the potential high area of contact between electrolyte and powder, which increases the diffusion rate of the ions into the material, and the consequent adaptability for mass production of graphene. The main limitation of this design is that no space is given to the graphite to expand during exfoliation. Therefore, if the vertical force applied by the load is higher than the expansion force of the graphite, this would probably not happen, and only excessive oxidation will be given in the material. Hence, a posterior sonication phase is required in order to obtain graphene oxide. Figure 23 illustrates the half cut of this design.

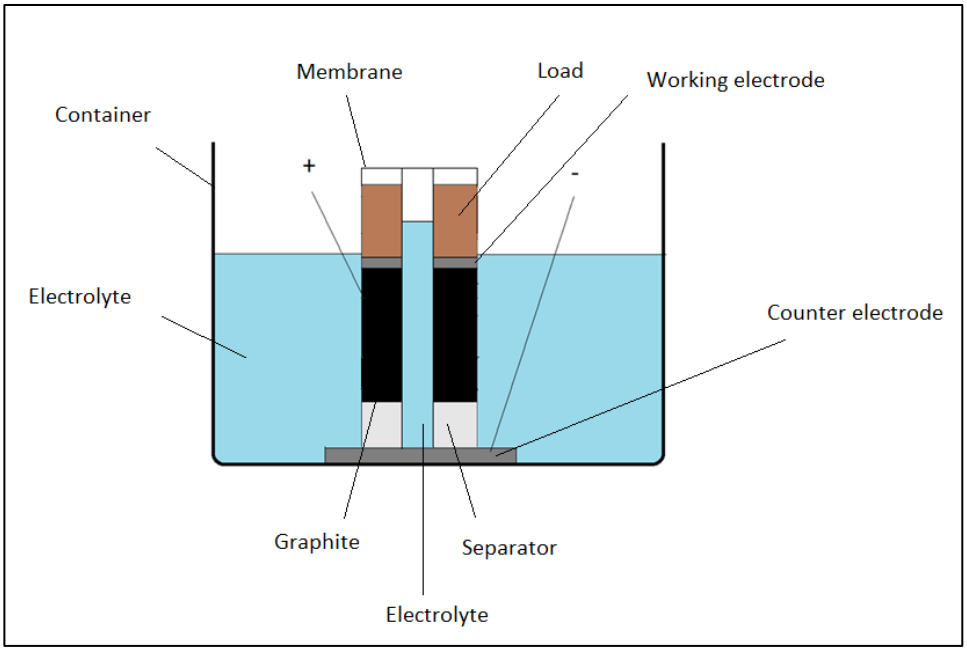

Figure 23: Cylinder design half cut

3.1.5 Pressurized design

All the previous proposed solutions are based on the introduction of an external force that compresses the powder. On the one hand, a system rotation which induces a centrifugal force that pushes the flakes towards the container walls. On the other hand, a superior load, that helped with gravity, compresses the material in the downward direction. Both designs need an external body or energy to provide the required state of the graphite powder. However, none of them take advantage of the own process to obtain this compression.

Here, a novel design that uses internal forces to induce the necessary electrical connection between the different flakes is presented. During the electrochemical exfoliation process, gases are liberated from both the anode and the cathode as a result of the oxidation and reduction process. Moreover, when stable materials are used as feeder electrodes, this gas creation process happens as long as the voltage is still being applied.

This approach tries to take advantage of this fact by sealing the top cover of the cylinder. Hence, the gas liberated from the anode will be trapped in this volume, increasing then the pressure and, consequently, generating a downward force that compresses the flakes. Furthermore, this approach also deals with the main disadvantage of the design proposed in chapter 3.1.4, which is the lack of free space for graphite expansion.

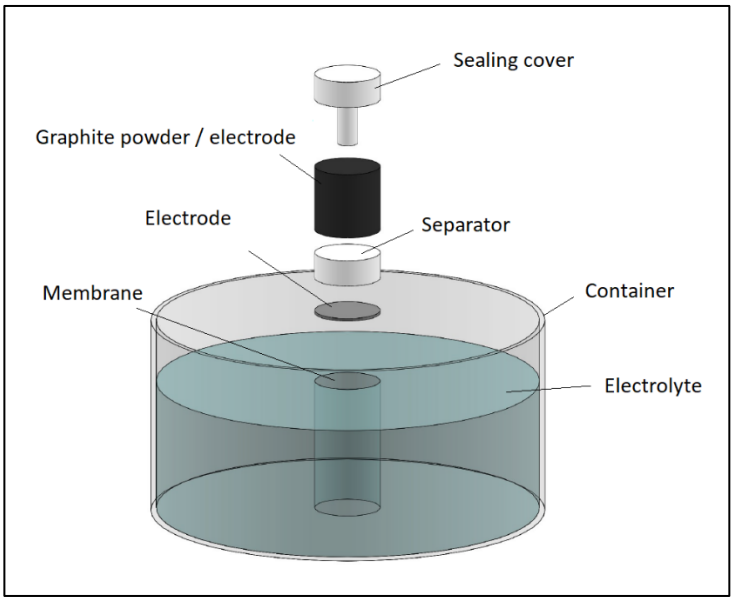

Figure 24: Pressurized design

The advantages of this electrochemical set-up are several. First, as explained before, this design does not disturb the expansion process of the graphite. Also, this design is suitable for mass production of graphene by implementing the inner cylinder improvement. Another benefit is that the vertical load which is applied over the graphite can be controlled by adjusting the pressure increment in the pressurized volume. However, this also represents a disadvantage when compared to other approaches because a method to control this pressure is required. For instance, a pressure valve where the user chooses the maximum pressure can be part of the upper sealing body. Moreover, the maximum possible

pressure applied also is limited by the membrane used on the configuration. While other compression methods only apply this force against one direction, the force generated by pressure is directly dependent on the area where the pressure acts. For instance, in the proposed design, the force over the graphite is:

$$F_g = \frac{\pi P D}{4} \tag{7}$$

Where P is the pressure created by the gases, and D is the diameter of the cylinder. In addition, the force that the membrane holds is:

$$F_m = \pi D H P \tag{8}$$

Being D the diameter of the cylinder, H the vertical distance between the lower surface of the cover and the upper surface of the graphite, and P the pressure on this volume. Therefore, the permeable container has to withstand the force Fm. Figure 25 shows a half cut illustration of the cell where the free space that will increase in pressure can be observed.

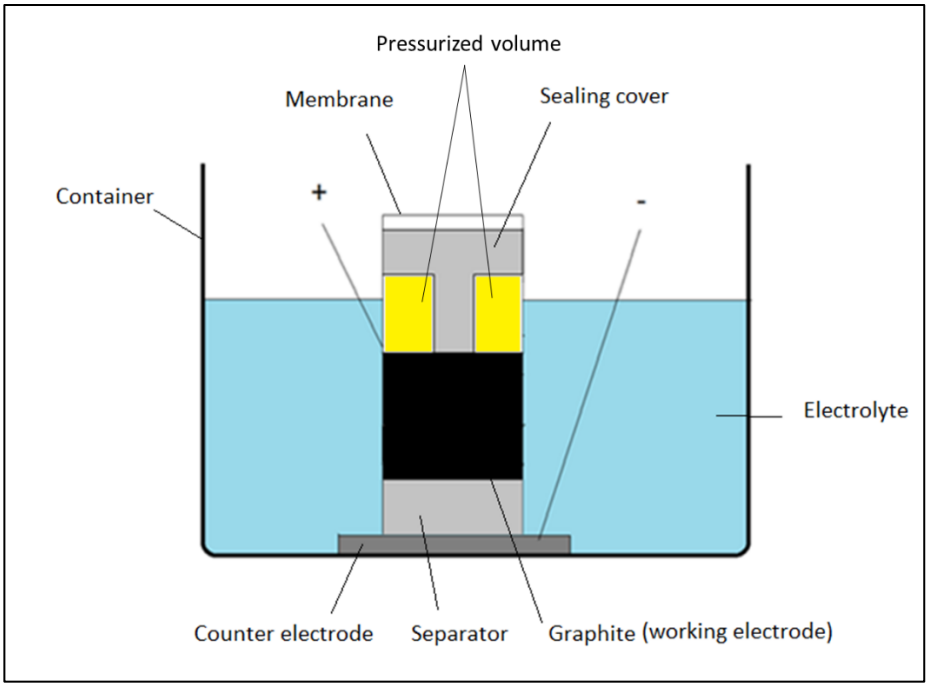

Figure 25: Pressurized design half cut

3.2 Methodology

This section is intended to explain the methodology followed to test part of the proposed designs presented above. Different experiment parameters such as the used electrolyte or the applied voltage during the electrochemical process are discussed here.

3.2.1 Tested designs

First, due to time and physical laboratory constraints, only a few of the proposed designs are actually built and tested. All the designed electrochemical cells are:

Table 1 - Proposed designs

Order	*Design*	*Tested*	*Reason*
1	Centrifugation-assisted	No	Lab constraint
2	Centered	No	Cost
3	Bipolar	No	Safety
4	Cylinder type	Yes	Simplicity
5	Pressurized	Yes	Simplicity

Firstly, the centrifugation-assisted design has several physical limitations that cannot be addressed in the laboratory. For instance, the connection type between DC supplier and the electrodes is not as trivial as in other approaches. Also, a centrifugate which is able to rotate the whole system is required, and currently, is not available in the used installations. Secondly, the centered design requires a large amount of material to work as a counter electrode. Normally, platinum is used as the electrode, but it is a precious material with a high cost. Nonetheless, other cheaper materials that are stable against a reduction process can be used as cathode in the electrochemical process, such as titanium. Therefore, other designs were considered to be designed in first order due to preferable conditions. Finally,

the bipolar alternative was also dismissed because it could not be carried out under safe conditions. This process demands voltages which can surpass 250 V and even 1,000 V, which cannot be reached by the current Keithley 2400 source meter of the ESCL laboratory[45].

On the other hand, the last two proposed cells have been built and tested under certain conditions that are explained in section 3.2.3. These were chosen because it was understood they were the simplest designs. Figure 26, Figure 27 and Figure 28 show the tested designs. The first two set-ups are different variations of the cylinder type design, where both the load and the separator are formed of polyvinyl chloride (PVC). On the one hand, the photograph shown in Figure 26 uses a titanium plate to bring electrical connection to the graphite powder. Furthermore, a titanium wire is connected using a fit interference with the circular plate that is located over the flakes. This wire is directly connected to the source meter using an alligator clip. However, after several trials, it was observed that the redox process lost efficiency. This was easily found by noticing a reduction in the gas generation on both electrodes. Consequently, the exfoliation of graphite was not taking place. Finally, after studying the possibilities, it was detected that the titanium plate suffered from oxidation, which affected the efficiency of the electrochemical process.

Figure 26: Cylinder type design with titanium

Therefore, the connection between the source meter and graphite required a new medium. Luckily, this issue was quickly solved by replacing the titanium plate with a platinum wire. However, the plate could not be used to evenly press the graphite powder anymore. Hence, the load adopted this new task in the configuration. Therefore, this PVC rod served as both a compressive force and a graphite leveler, as it can be observed in Figure 27. Once the platinum wire was installed, the reduction-oxidation process happened uninterruptedly while the voltage was applied. Although the titanium was replaced due to its vulnerability against oxidation, it is stable against a reduction process. Thus, this material was used as cathode in all the following experiments.

Figure 27: Cylinder type design with platinum

Additionally, the pressurized design follows the same configuration as the previous presented set-up. Hence, a platinum wire is used to provide electrical connection to the graphite powder. Moreover, the layout varies when compared to the other designs. As Figure 28 shows, the free space that allows the expansion of graphite is created by introducing a vertical PVC rod between the material and the PVC load. This body that was previously used as load was transformed into the sealing cover by adding two rubber bands that ensured the perfect joint between membrane and cover. At the same time, the identical procedure was followed in the separator, which acted as a sealing body too.

Figure 28: Pressurized design model

3.2.2 Parameter selection

3.2.2.1 Electrolyte

This subsection presents a discussion on the type of electrolyte that is used in the designs. Several types of electrolytes are usable for the electrochemical process. However, the most commons ones are ionic liquids, aqueous acids, and aqueous inorganic salts. Parvez et al.[46] presented inefficient results of exfoliation under ionic liquids where the resulting graphene was characterized by low lateral size and inappropriate electronic properties. Furthermore, the process yield was too low compared to other electrolytes. On the other hand, acids can provide high exfoliation rates, but the quality of the graphene is not optimum. This is caused because of the strong oxidating power of the agent, which causes fast exfoliation and, therefore, the separation of non-completely exfoliation graphite flakes from the working electrode[47]. Finally, past research has proven that aqueous

inorganic salt electrolytes reduce the number of oxygen groups in the graphene while it maintains similar yield than those achieved with acid electrolytes[46]. Some examples of the different possible electrolytes are:

- Ionic liquid: N-butyl, methylpyrrolidiniumbis (trifluoromethylsulfonyl)-imide.
- Acidic solutions: sulfuric acid (H_2SO_4), Sodium hydroxide (NaOH), phosphoric acid (H_3PO_4).
- Inorganic salts: ammonium sulphate ($(NH_4)_2SO_4$), sodium sulfate (Na_2SO_4).

With this in mind, the aqueous inorganic salt ammonium sulfate electrolyte is chosen to be implemented in the design.

Finally, the last electrolyte parameter that needs to be addressed is the molarity of the solution. The electrochemical process starts by applying a voltage between the electrolytes, which causes the reduction of water in the cathode. After that, these hydroxyl ions (OH^-) attack the grain boundaries of the graphitic structure. This generates an interlayer expansion that allows the sulfate ions (SO_4^{2-}) intercalation between the 2D layers. Finally, the reduction of this sulfate ions and the water oxidation produce gasses (SO_2 and O_2) that finish the separation process of the layers. Hence, an equilibrium between the amount of water and inorganic salt must be found in the solution to succeed in the exfoliation process presented above. Parvez et al. [46] studied the effects on the process of the ammonium sulfate electrolyte concentration. It was concluded that molarities below 0.1 M and above 1 M resulted inefficient due to the lack of hydroxyl ions or sulfate ions, respectively.

Past research has proven that 0.1 M to 1 M $(NH_4)_2SO_4$ aqueous sulfates present the best results regarding graphene. Therefore, the selected solutions that are used in the process are: 0.1 M $(NH_4)2SO_4$ and 0.5 M $(NH_4)_2SO_4$.

3.2.2.2 Voltage

Apart form molarity, the other main parameter of the process is the voltage applied and the duration. Nurhafizah et al.[48] studied the different effects this variable generated in the overall process. Voltages of 3, 5, 7, 10 and 12 V were applied for 24 hours cycles. Results showed that voltage below 7 V did not effectively exfoliate the graphite rod due to the lack of oxidation. On the other hand, using 12 V generated a high defect graphene oxide which was induced by a high oxidizing power, so a meaningful percentage of oxygen groups were found in the final product. On the other hand, while 7 V produced stacked graphene oxide layers, 10 V added the necessary oxidation to the process to successfully obtain few-layer, high quality graphene.

Hence, two voltages are chosen to be used in the proposed process: 10 V and 20 V. The duration of the voltage application is set at 60 minutes. In addition, a prior intercalation step with a lower voltage (2 V) is included. In order to study the effect of this factor, the time duration varies between 10 minutes and 30 minutes.

3.2.3 Procedure

This subsection presents the followed test procedures including the selected parameters for each of the cycles. Although there are parameters variability in this part of the project, the general followed procedure has been the same for all the trials. Table 2

summarizes the order and the description of the followed steps to produce graphene using any proposed design.

Table 2: Process' steps

	Step	*Description*
1	Select initial graphite	Use high precision balance to get 1000 mg of graphite powder
2	Set-up building	Prepare the appropriate design using source meter, physical elements of the design, electrolyte, and graphite
3	Intercalation	Apply 2 V for the desired time
4	Exfoliation	Apply the desired exfoliation voltage for 60 minutes
5	Vacuum filtration	Vacuum filter the exfoliated graphite using a 0.2 µm pore size nylon filter
6	Drying process	Air dry the sample for 24 hours

Table 2 continued

7	Dispersion	Disperse the sample in 500 mL of dimethylformamide (DMF)
8	Sonication	Sonicate the bottle containing the DMF solution for 30 minutes
9	Graphene separation	Wait 120 hours to let the graphite deposit at the bottom of the bottle
10	Filtration of DMF solution	Vacuum filter 50 mL using a 0.2 μm pore size nylon filter[49]
11	Graphene characterization	Prepare the samples for characterization

Only steps 2, 3 and 4 change depending on the selected parameters for each of the experiments. Step 10 conglomerates the different procedures that are needed for each of the characterization methods. More specifically, due to the lack of time, only XPS and Raman spectrometry have been used to study the graphene of each of the cycles. In order to prepare the samples, part of the graphene obtained in step 9 is dispersed in ethanol using ultrasound sonication for 15 minutes. Afterward, 1 mL of the ethanol solution is drop

casted over a glass plate and is oven dried at 40 °C. This procedure is repeated 5 times in order to increase the graphene on the surface, so that more graphene flakes can be studied during the characterization process. Finally, these samples are introduced into the characterization equipment.

Also, in order to promote ion diffusion through the graphite powder, electrolyte has been added into the cylinder created by the membrane container. In the first case, where a physical load compresses the powder, 10 mL are introduced in the cylinder. As graphite powder sinks, it is deposited over the separator, so the amount of electrolyte does not need to be specific. While all the powder remains under the surface of the electrolyte, it helps the ion diffusion. However, in the pressurized case, the amount of electrolyte must be controlled because a liquid medium has an immutable pressure. Therefore, if the graphite powder is located below the electrolyte's surface, it is not compressed by the higher pressure generated by the gasses generated in the anode. Hence, in order to effectively compute both the material compression and the ionic diffusion, the graphite powder can be wet, but no gas-liquid interface can be generated.

In addition, the source of errors related to the proposed procedure are discussed. First, in the electrochemical exfoliation process (step 1 – step 4), a weight measuring error might be included due to the own balance error[50]. Furthermore, in the following steps, the powder (graphene and graphite) manipulation increases the chances of adding a higher error term to the yield calculations shown in chapter 4. For instance, the smaller exfoliated graphene flakes might get stuck into the filters used in steps 5 and 10. This fact is directly related to the porous size of the filters as well as the hydrophilic nature of graphene[51], which is the

same of the filters, as furtherly explained in chapter 4. Also, these smaller flakes are difficult to physically manipulate in order to, for example, transfer them from one container to another. External factors such as a small air stream might influence these processes.

Table 3 presents the different tests that have been carried out and the specific parameters for each one.

Table 3: Laboratory tests

Case	*Design*	*Electrolyte*	*Int voltage / time*	*Exf voltage / time*
1	Load	0.1 M $(NH_4)_2SO_4$	2 V / 10 min	10 V / 60 min
2	Load	0.1 M $(NH_4)_2SO_4$	2 V / 10 min	20 V / 60 min
3	Load	0.1 M $(NH_4)_2SO_4$	2 V / 30 min	10 V / 60 min
4	Pressurized	0.1 M $(NH_4)_2SO_4$	2 V / 30 min	10 V / 60 min
5	Pressurized	0.1 M $(NH_4)_2SO_4$	2 V / 10 min	20 V / 60 min
6	Pressurized	0.5 M $(NH_4)_2SO_4$	2 V / 10 min	10 V / 60 min

Finally, Figure 29 presents the general set-up which was used in all the tests.

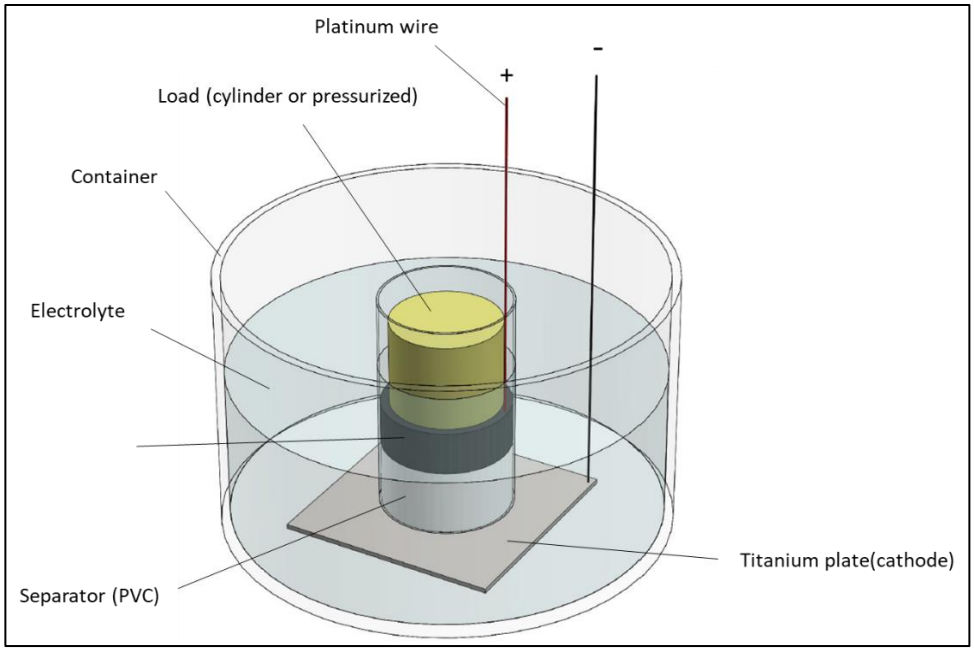

Figure 29: General electrochemical cell set-up illustration

Additionally, it is worth mentioning that the development of this project has been affected by external uncontrollable factors that have disturbed the initial planning. In particular, the coronavirus outbreak postponed the experiment part of the project, which has shortened the number of tests that were initially intended to be performed. Ideally, in order to maximize accuracy, each of the cases with specific conditions should have been repeated several times. By doing this, an average and variation of each of the calculations presented in chapter 4 could have been calculated, and therefore, the conclusions could have been precisely determined.

4 RESULTS AND DISCUSSIONS

This chapter presents a discussion on the result of each of the tried experiments. First, the yield of each of the different electrochemical exfoliation processes are calculated to obtain which conditions are more favorable for graphene production when graphite powder is the precursor material. Afterward, to complete previous yield conclusions, the characteristics of the product are studied to determine the quality of each design's final product. Both Raman spectrometry and X-Ray photoelectron spectroscopy (XPS) are used to characterize the graphene.

The main objective of this project is to design an electrochemical cell which is capable of exfoliating graphite powder in an efficient way in order to overcome this well-known process limitation. Therefore, the first logical step to prove this is to calculate the overall process yield.

Several methods exist to obtain the yield of a process. For instance, one of the most common approaches to address this parameter is to measure the weight of the produced graphene and compare it to the initial graphite weight, 1 gram in this case. However, when this method was tried, several issues were found. Graphite is known to be a hydrophobic material, so it repels water. Therefore, after vacuum filtration on a hydrophilic filter, such as nylon filters, it can be easily separated after it dries. However, although the common belief was that graphene followed this same nature, it has been recently proved that, in reality, graphene is hydrophilic[51]. This represents a limitation to the proposed yield calculation approach explained above because if graphene and filter share their nature, the

filtration process sticks both materials together. In fact, the hydrophilic nature depends on the thickness of the graphene flakes, being a monolayer hydrophilic, while a multilayer is hydrophobic as it is basically a small flake of graphite oxide. Hence, after the sample dries after filtration, the thinnest layers are attached to the filter, while the thickest particles can be detached. Thus, if the graphene mass is measured after the filtration, the calculated yield is not reliable. A proposed alternative was to measure the filter weight before and after filtration, so that the mass difference would be the graphene's mass. Nonetheless, this approach was tried and a negative mass value between both samples was finally measured. This event can be explained due to the corrosive nature of the used organic solvent (DMF) or due to the loss of molecules that were hidden inside the filter during the filtration. Another influential factor that can bring errors to the yield calculation is the own precision balance[50]. This equipment uses torque to weigh the samples. Therefore, if the position of the sample changes, the measurement changes. This fact limits other calculations approaches, such as using the solution density to directly calculate the yield by measuring the weight difference between this solution and pure DMF.

Finally, the yield calculation was carried out by measuring the graphite powder which precipitated in the DMF solution. From the initial volume of 500 mL of solution, the top 450 mL solution, which only has dispersed graphene, are moved to an empty container. This remaining 50 mL of DMF solution has both the bottom graphite and some dispersed graphene. Therefore, after considering a homogeneous dispersion of graphene in DMF, a correction variable γ can be calculated by:

$$\gamma = \frac{V_o}{V_o - V_f} = \frac{500\ mL}{(500 - 50)\ mL} \tag{9}$$

$$\gamma = 1.11 \tag{10}$$

This approach is considered to increase the accuracy of the yield calculation because the yield is expected to be lower than 50% and, the higher the measurable mass, the lower the relative error associated with the calculation. This means that as the graphene mass is going to be lower than the final non-exfoliated graphite mass, the inevitable process error has a smaller influence when the higher mass is used to run the yield calculation.

The weight measurements and the obtained yield of the different cases are shown in Table 4.

Table 4: Processes' yield

Case	*Total mass*	*Graphene mass*	*Corrected mass*	*Yield*
1	803.52 mg	196.48 mg	218.09 mg	21.81 %
2	855.98 mg	144.02 mg	159.86 mg	15.99 %
3	828.72 mg	171.28 mg	190.12 mg	19.01 %
4	825.80 mg	174.20 mg	193.36 mg	19.34 %
5	848.10 mg	151.90 mg	168.60 mg	16.86 %
6	831.75 mg	168.25 mg	186.76 mg	18.68 %

As explained in Table 3, cases 1,2 and 3 apply the load design, while cases 4,5 and 6 are based on the pressurized approach. First, a comparison between the cases of each of the designs is discussed, which is followed by a general discussion comparing both designs.

The first proposed electrochemical cell uses the gravity to compress the graphite powder with a top load. Between the three experiments that uses this method, the first one presents the best results in terms of yield, with a near 22%, followed by case 3, with a 19%, and, finally, case 2, with 16%. In this case, the two variations that are introduced between case 1 and cases 2 and 3 is the increment of exfoliation voltage from 10 V to 20 V in case 2 and a longer intercalation step, which was initially set on 10 minutes, while in case 2 is prolonged to 30 minutes. As data demonstrates, doubling the voltage reduces almost in a 6% the process yield, which, in relative terms, means a reduction of a relative 27% when compared to the yield of case 1. This abrupt reduction of yield is caused by an excessive oxidizing power that speeds up the exfoliation process but deteriorates the graphene by introducing anexcessive amount of oxygen groups into the material. This extra oxygen composition increases the Van der Waals attraction force between the graphene oxides flakes, which easiest the sheets agglomeration[48,52,53]. This union increases the particle's mass, which drives their precipitation from the DMF solution to the bottom of the container. On the other hand, when the intercalation period is increased, the yield also decreases. Previous work on this matter[54,55] show that the period with low voltage bias wet the sample, facilitating thus the SO_4^{2-} ions interlayer intercalation. However, this pre-exfoliation step is usually not longer than 10 minutes because at some point, the excessive intercalation process at low voltage lowest the exfoliation capacity of the process.

In the second case, when the graphite compression is achieved by increasing the pressure of the chamber, the effects of the intercalation duration, the applied voltage, and the electrolyte molarity are studied. Here, applying the intercalation voltage bias during 30 minutes, a 10 V voltage for the exfoliation for 60 minutes, and a 0.1 M electrolyte provide the best yield results. Again, when the high voltage vias is doubled, a significant yield reduction is given, which is explained following the above reasoning. Moreover, these three cases allow us to explore the effects of the electrolyte concentration on the process efficiency. Results show that increasing the concentration from 0.1 M to 0.5 M improves the yield when compared to case number 5, where 20 V are used in the exfoliation step. However, the 18.7% of yield is not sufficient to obtain better results than in case number 4. When graphite powders are used instead of a monolithic graphite body, the contact surface between the electrolyte and the material increases. Generally, when a graphite plate or rod is exfoliated, this process starts from outside to inside of the part as the electrolyte provides ions to the interference surface. In powders, on the other hand, despite being compressed to ensure electrical connection, this contact area is always larger because the graphite particles that conform the powder are not physically connected. Therefore, although contact is provided by a pressure, free spaces remain between the particles, which is filled up with electrolyte. In monolithic structures, the concentration of the electrolyte must be balanced to provide both a grain boundary deterioration, and an effective interlayer ion intercalation[46,56]. For instance, the optimum concentration when $(NH_4)_2SO_4$ electrolyte is used is established between 0.1 M and 1 M. Nevertheless, as the surface of contact between electrolyte and material increases in powders, more OH^- ions are needed to attack the grain boundaries in order to facilitate the SO_4^{2-} ion intercalation. Consequently, the

ideal concentration is lower than in the previous case. This comparison proves that 0.5 M electrolyte worsens the results ofthe 0.1 M electrolyte process, so the finest concentration is lower than 0.5 M. Nonetheless, these results provide a non-deterministic answer to the most efficient concentration question, so further optimization is required to accurately determine this value.

Finally, both designs' results are compared. Between all the cases, the one which provides the highest yield is the first one, with 0.1 M $(NH_4)_2SO_4$ electrolyte, 10 minutes for intercalation duration, and 10 V as exfoliation voltage as parameters. However, for the lack of time, these parameters have not been tested using the other proposed electrochemical cell. Therefore, the other trials should provide more details about which design is preferable for future analysis. Cases 3 and 4 and cases and cases 2 and 5 share the same experiment conditions, so they can be directly compared. In both cases, the pressurized design provides better results, improving results by 0.33% and 0.87%, respectively, or, in relative terms, by ~2% and ~5.5%. Hence, this trend can be extrapolated to the other cases with specific conditions that have not been carried out in both designs. This means that in overall terms, the pressurized proposed electrochemical set-up presents a higher yield than the load design.

Although it has been demonstrated that the pressurized design presents a higher exfoliation efficiency, the graphene characterization is needed in order to determine the product quality of both designs and, therefore, discuss if one cell is superior to the other one.

XPS was used to study the chemical composition of the different experiment samples. Here, the Cs spectrum is formed by the following peaks: sp^2 bond (C=C) at 284.5 eV; sp^3 bond (C-OH) at 285.4 eV; C-O-C at around 286.4 eV; C=O at around 287.1 eV; and finally, O-C=O bond at 287.1 eV [57,58].

As the procedure followed in the yield discussion, first the three cases from both designs are commented separately. Afterward, both designs are globally compared to determine the global results of both processes.

First, in the load case, high resolution XPS spectra of the C1s peak is shown in Figure 30.

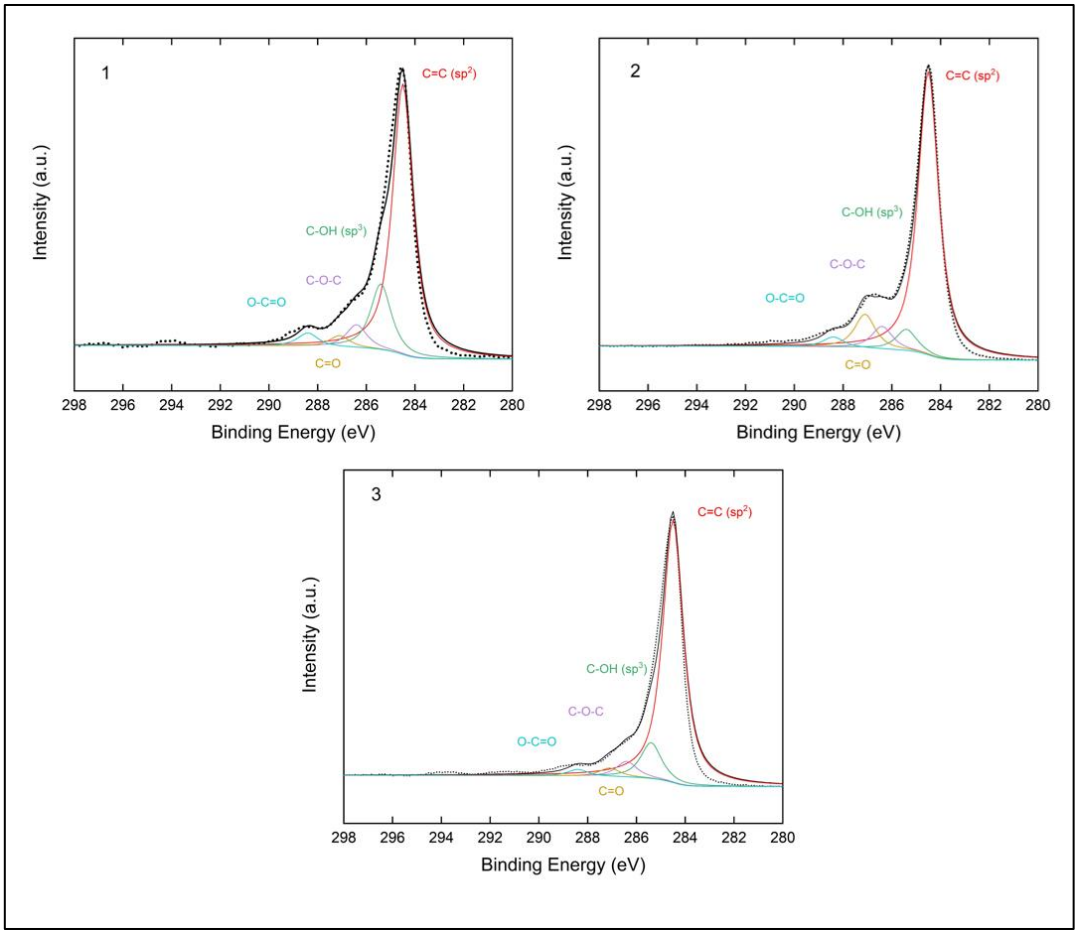

Figure 30: High resolution XPS of the C1s peak for cases 1,2 and 3

Furthermore, the result of the deconvoluted XPS for cases 1, 2 and 3 is:

Table 5: Deconvoluted peaks in cases 1,2 and 3

Case	*C=C*	*C-OH*	*C-O-C*	*C=O*	*O-C=O*
1	70.4%	17.1%	6%	2.9%	3.4%
2	76.3%	5.8%	6.1%	9.1%	2.7%
3	79.7%	10.9%	4.8%	2.6%	2%

As it can be inferred from Table 5, the C=O signature significantly increases when the exfoliation process voltage increases from 10 to 20 V. Also, a significant variation in the C-OH signature is observed between case 1 and cases 2 and 3.

On the other hand, the deconvoluted XPS spectrum for the pressurized case is presented in Figure 31.

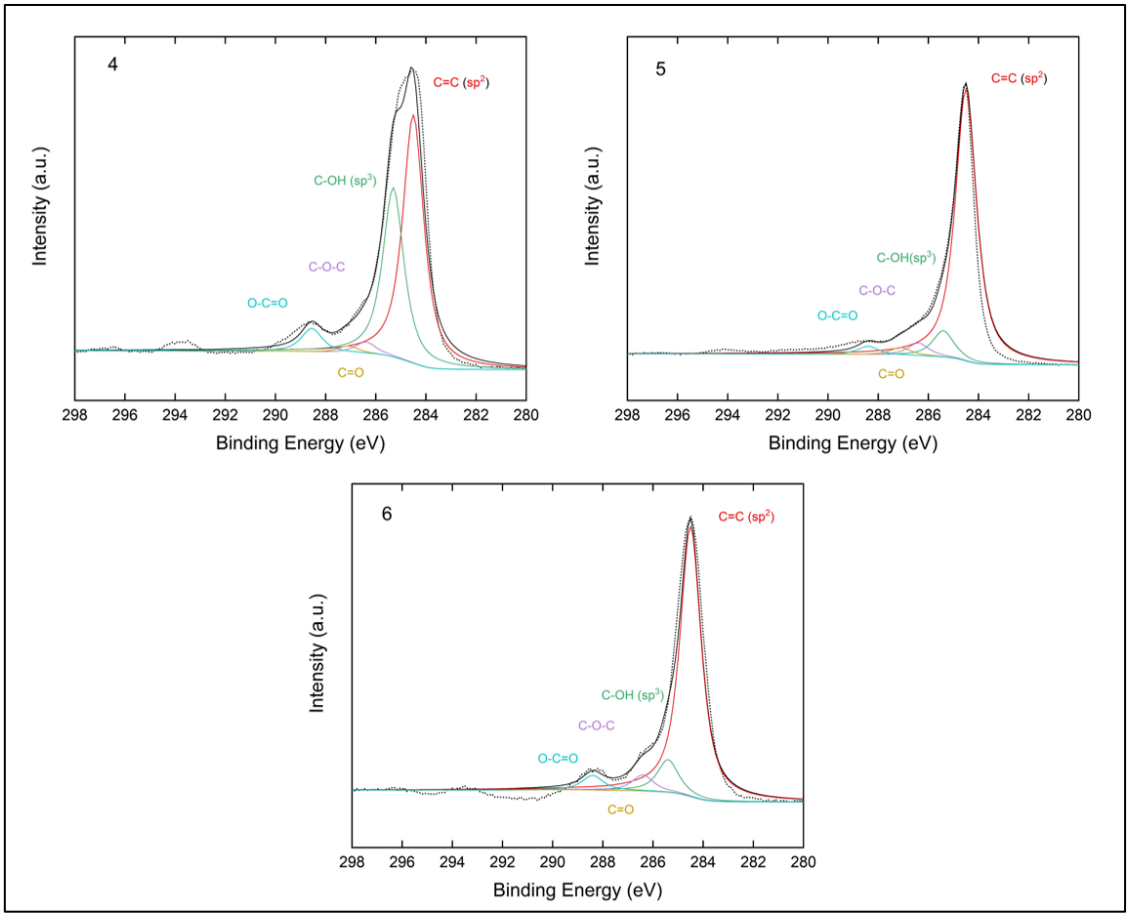

Figure 31: High resolution XPS of the C1s peak for cases 4,5 and 6

These experiments present the following deconvoluted XPS results, which show the different functional groups which are found in the graphene:

Table 6: Deconvoluted peaks in cases 1,2 and 3

Case	*C=C*	*C-OH*	*C-O-C*	*C=O*	*O-C=O*
4	54%	36.8%	2.6%	1.5%	5.1%
5	83%	8.1%	3.9%	2.4%	2.6%
6	81%	9.8%	4.8%	0%	4.4%

Here, while cases 5 and 6 show similar results, case 4 has an extremely low C=C 54 atom% and a remarkable C-OH presence of ~37 atom %.

Krishnamoorthy et al.[59] studied the implications of the degree of oxidation in the structure of graphene. Their project demonstrated that with relatively low oxidation levels, the hydroxyl and carboxyl groups increase, whereas at high oxidation rates, a reduction of these groups is given. Therefore, cases 1 and 4, which present the higher hydroxyl and carboxyl atom%, correspond to a low oxidation rate. This could mean that the obtained samples in these cases are not graphene oxide, but graphitic oxide. However, this research was focused on the production of graphene using chemical exfoliation. Hence, high oxidation rates were needed to successfully generate graphene. On the other hand, as explained in section 2.1.6, the electrochemical process does not require this level of oxidation in order to obtain high quality graphene. This means that despite the fact that cases 1 and 4 are less oxidized, this oxidation level can be enough to achieve the exfoliation of the pristine powder. In fact, the specific conditions of these two experiments report the best yield.

Finally, Raman spectrometry is applied in order to determine the quality of each of the different proposed cells and parameters. First, the Raman spectrum from the pristine graphite powder is provided in Figure 32 in order to realize and understand the given change in each of the designs.

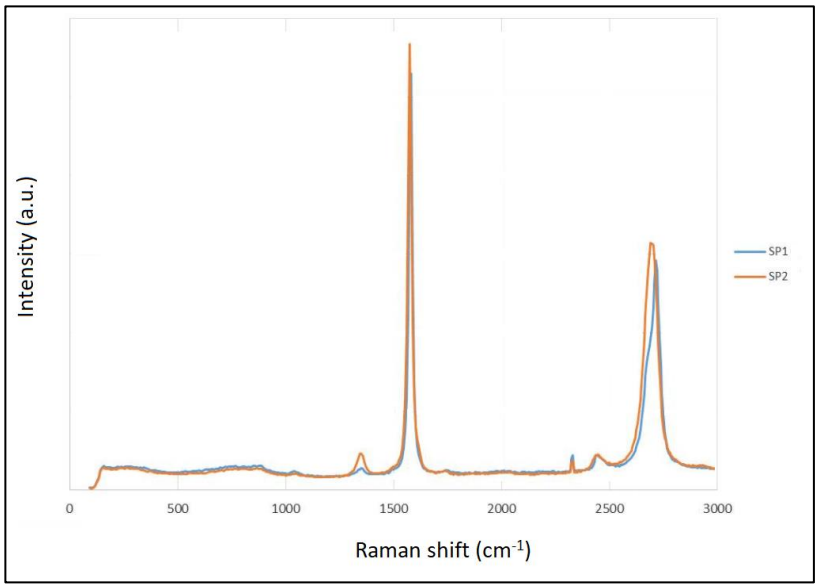

Figure 32: Raman spectrum for the pristine graphite powder[60]

Firstly, the graphene from the loaded design is characterized using Raman spectrometry with a 488-nm excitation laser. Figure 33 shows the Raman spectrum for the first three cases. Normally, graphene displays a D peak of ~1350 cm^{-1}, G peak at ~1580 cm^{-1}, and a 2D peak at ~2680 cm^{-1} [37]. With this in mind, it can be observed in the different spectrum diagrams that these peaks are actually given in all the proposed cells.

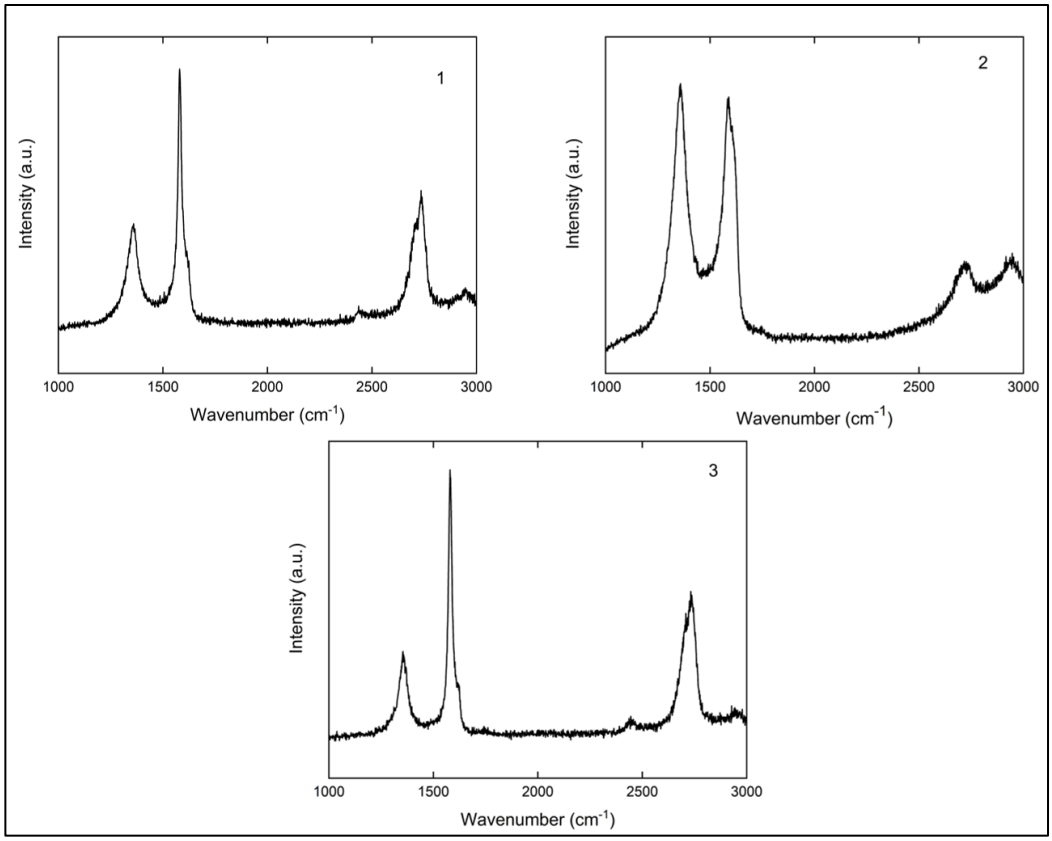

Figure 33: Raman spectrum for cases 1,2 and 3

Additionally, Table 7 provides the calculated D peak to G peak and 2D to G peaks ratios.

Table 7: I_D / I_G and I_{2G} / I_G ratios for cases 1, 2 and 3

Case	I_D / I_G	I_{2D} / I_G
1	0.43	0.55
2	1.04	0.41
3	0.34	0.56

Raman spectrometry is an approach that allows to investigate the graphitic defects that exist in the structure by the D band that appear on the spectrum[61]. Therefore, the ratio I_D/I_G is directly related to the quality of the graphene, so if the ratio decreases, the quality improves. Results show that cases 1 and 3 present the best quality of graphene. Case 2, on the other hand, has a D to G ratio of 1.04, which is more than twice the number 2 case ratio and three times more than case 3 ratio. Here, the 20 V bias increases the abruptness of the process, deteriorating thus the quality of graphene. Furthermore, Raman spectrum 2D peak can be directly related to the material thickness[62].[63]these modifications Hence, a few-layer graphene spectrum presents a non-intense 2D peak with more than 5 layers. In the three presented experiments, these I2D/IG rates are above 0.4, which is relatively high for graphene.

On the other hand, results from the pressurized design are shown in Figure 34 and Table 8.

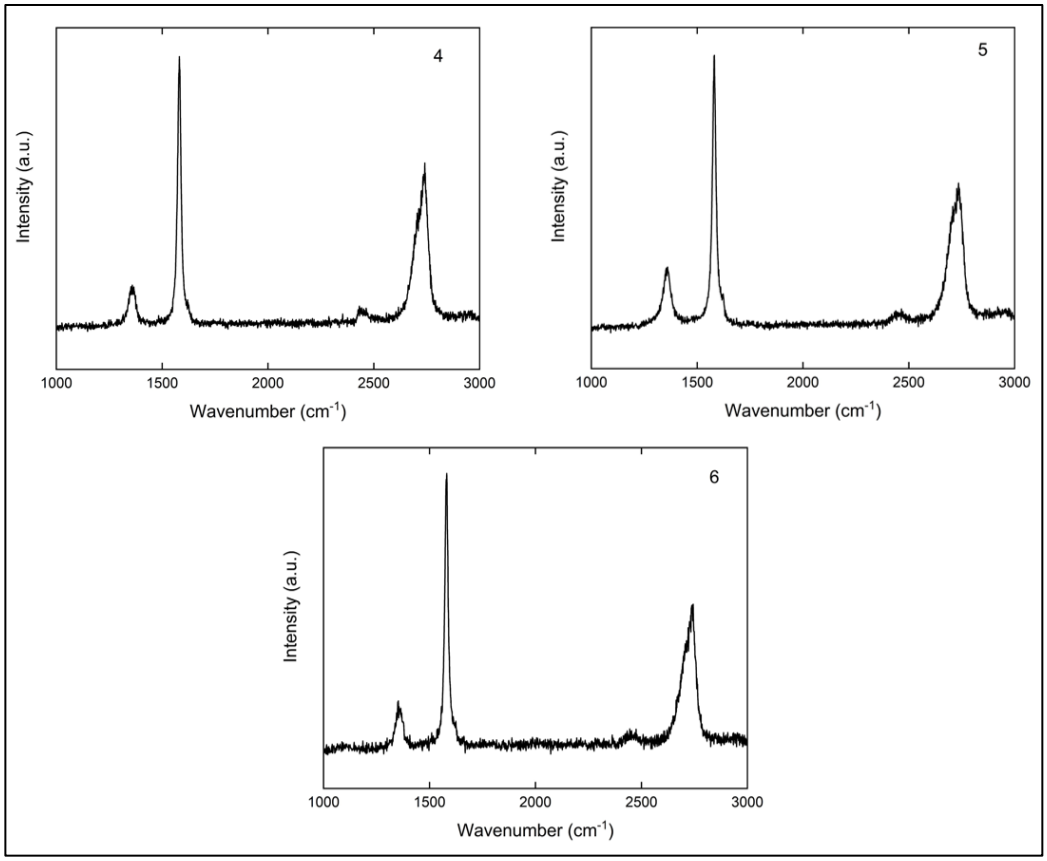

Figure 34: Raman spectrum for cases 4,5 and 6

Table 8: I_D / I_G and I_{2G} / I_G ratios for cases 4, 5 and 6

Case	I_D / I_G	I_{2D} / I_G
4	0.18	0.62
5	0.24	0.54
6	0.22	0.55

In this case, all the results indicate that a high-quality graphene is obtained due to the low D to G ratios. However, the thickness related ratio, the 2D to G, shows results that are comparable to the pristine graphite ratios.

Raman spectrometry proves that a thick material is obtained as a result of both proposed designs. In fact, it is likely that the final product is expanded graphite oxide instead of graphene oxide. Furthermore, this outcome explains the low oxygen functional groups which are present in the material, as XPS results prove. Finally, despite the valid yield calculation, the result may not be accurate due to the dispersion of both few-layer and multi-layer graphene particles.

Finally, in order to corroborate the results presented above, at least AFM is required. However, due to the lack of time, this characterization process was not carried out.

These results may be explained by the lack of compression of the graphite, which has caused the inefficiency of the exfoliation process. In the first case, the used load probably has not provided enough vertical force to ensure the electrical connection between particles. Moreover, as the process happens, the anode gas liberation might have continuously caused a migration of the graphite flakes despite the top load. On the other hand, the pressurized design lacked a necessary optimization process. For instance, the amount of electrolyte inside the membrane requires to be optimized in order to not interfere in the compression of the graphite. Furthermore, the pressure generated by the anode gasses might have not been enough to provide a notable compression. A pressure valve can be introduced in this design to improve the pressure control and, therefore, the process efficiency. Also, despite the characterization results, this novel idea of using the own

electrochemical process to address the compression problem conforms a potential base for future research on this area.

5 CONCLUSION

In summary, different designs of a cost-efficient electrochemical cell were proposed to address the exfoliation of graphite powder, which has become a process' limitation over the last years. Furthermore, two proposed approaches have been followed in order to physically build a model of the electrochemical set-up to test the model's capability to exfoliate graphite powders. In addition, a parameter variation study has been developed to investigate which conditions are more favorable to the exfoliation process, including electrolyte type and molarity, applied voltage for the intercalation and exfoliation steps, and the duration of the process steps. Finally, the graphene oxide under each specific condition has been characterized using X-ray photoelectron spectroscopy (XPS) and Raman spectrometry.

Graphene oxide characterization shows an overall low final product quality caused by the inefficient ion intercalation. Up to 22% process yield of multi-layer graphene oxide is obtained using the proposed designs. Moreover, when the graphite powder is compressed by a load, high oxidation without exfoliation is given because the setup does not provide enough space for the natural expansion of the material. Therefore, the alternative design where the chamber is pressurized using the electrochemical gasses shows higher potential improvements. However, although it shows slightly better yield results, the Raman spectra show thicker graphene flakes, which indicates that the used parameters on the pressurized designs present a lower exfoliation capacity than those used in the loaded design. These conclusions are based in a non-significant experimental sample size, so they are determined

under the hypothesis that the presented results are correct. Therefore, further experimentation is required in order to completely support these conclusions.

This project scope was focused on designing an electrochemical cell that overcomes the graphite powder exfoliation limitation of previous work. Indeed, several proposals that intend to address this process disadvantage have been described and, in some cases, built and tested. Despite the final results, the mentioned approaches can lead to future research towards a promising outcome by improving and optimizing current designs.

RERERENCES

(1) Yang, G.; Li, L.; Lee, W. B.; Ng, M. C. Structure of Graphene and Its Disorders: A Review. *Sci Technol Adv Mater* **2018**, *19* (1), 613–648. https://doi.org/10.1080/14686996.2018.1494493.

(2) Nurhafizah, M. D.; Suriani, A. B.; Mohamed, A.; Soga, T. Effect of Voltage Applied for Graphene Oxide/Latex Nanocomposites Produced via Electrochemical Exfoliation and Its Application as Conductive Electrodes. *Diamond and Related Materials* **2020**, *101*, 107624. https://doi.org/10.1016/j.diamond.2019.107624.

(3) Castro Neto, A. H.; Guinea, F.; Peres, N. M. R.; Novoselov, K. S.; Geim, A. K. The Electronic Properties of Graphene. *Rev. Mod. Phys.* **2009**, *81* (1), 109–162. https://doi.org/10.1103/RevModPhys.81.109.

(4) Falkovsky, L. A. Optical Properties of Graphene and IV–VI Semiconductors. *Phys.-Usp.* **2008**, *51* (9), 887–897. https://doi.org/10.1070/PU2008v051n09ABEH006625.

(5) Brodie, B. C. XIII. On the Atomic Weight of Graphite. *Philosophical Transactions of the Royal Society of London* **1859**, *149*, 249–259. https://doi.org/10.1098/rstl.1859.0013.

(6) Boehm., H. P.; Clauss, A.; Fischer, G. O.; Hofmann, U. Dünnste Kohlenstoff-Folien. *Zeitschrift für Naturforschung B* **1962**, *17* (3), 150–153. https://doi.org/10.1515/znb-1962-0302.

(7) Novoselov, K. S. Electric Field Effect in Atomically Thin Carbon Films. *Science* **2004**, *306* (5696), 666–669. https://doi.org/10.1126/science.1102896.

(8) Nicholl, R. J. T.; Conley, H. J.; Lavrik, N. V.; Vlassiouk, I.; Puzyrev, Y. S.; Sreenivas, V. P.; Pantelides, S. T.; Bolotin, K. I. The Effect of Intrinsic Crumpling on the Mechanics of Free-Standing Graphene. *Nat Commun* **2015**, *6* (1), 8789. https://doi.org/10.1038/ncomms9789.

(9) Tour, J. M. Top-Down versus Bottom-Up Fabrication of Graphene-Based Electronics. *Chem. Mater.* **2014**, 163–171.

(10) Chua, C. K. Top-down Approach towards Graphene: Synthesis and Electrochemistry, Nanyang Technological University, 2013. https://doi.org/10.32657/10356/54864.

(11) Galstyan, V.; Bhandari, M.; Sberveglieri, V.; Sberveglieri, G.; Comini, E. Metal Oxide Nanostructures in Food Applications: Quality Control and Packaging. *Chemosensors* **2018**, *6*, 16. https://doi.org/10.3390/chemosensors6020016.

(12) Sinclair, R. C.; Suter, J. L.; Coveney, P. V. Micromechanical Exfoliation of Graphene on the Atomistic Scale. *Phys. Chem. Chem. Phys.* **2019**, *21* (10), 5716–5722. https://doi.org/10.1039/C8CP07796G.

(13) GLAB-Labortaroty for graphene. Exfoliation and Lithography, Microchemical Exfoliation http://www.graphene.ac.rs/exfoliation.html.

(14) Hernandez, Y.; Nicolosi, V.; Lotya, M.; Blighe, F. M.; Sun, Z.; De, S.; McGovern, I. T.; Holland, B.; Byrne, M.; Gun'Ko, Y. K.; Boland, J. J.; Niraj, P.; Duesberg, G.; Krishnamurthy, S.; Goodhue, R.; Hutchison, J.; Scardaci, V.; Ferrari, A. C.; Coleman, J. N. High-Yield Production of Graphene by Liquid-Phase Exfoliation of Graphite. *Nat Nanotechnol* **2008**, *3* (9), 563–568. https://doi.org/10.1038/nnano.2008.215.

(15) Bracamonte, M. V.; Lacconi, G. I.; Urreta, S. E.; Foa Torres, L. E. F. On the Nature of Defects in Liquid-Phase Exfoliated Graphene. *J. Phys. Chem. C* **2014**, *118* (28), 15455–15459. https://doi.org/10.1021/jp501930a.

(16) Skaltsas, T.; Ke, X.; Bittencourt, C.; Tagmatarchis, N. Ultrasonication Induces Oxygenated Species and Defects onto Exfoliated Graphene. *J. Phys. Chem. C* **2013**, *117* (44), 23272–23278. https://doi.org/10.1021/jp4057048.

(17) Flint, E. B.; Suslick, K. S. The Temperature of Cavitation. *Science* **1991**, *253* (5026), 1397–1399. https://doi.org/10.1126/science.253.5026.1397.

(18) Suslick, K. S.; Flannigan, D. J. Inside a Collapsing Bubble: Sonoluminescence and the Conditions during Cavitation. *Annu Rev Phys Chem* **2008**, *59*, 659–683. https://doi.org/10.1146/annurev.physchem.59.032607.093739.

(19) Polyakova (Stolyarova), E. Y.; Rim, K. T.; Eom, D.; Douglass, K.; Opila, R. L.; Heinz, T. F.; Teplyakov, A. V.; Flynn, G. W. Scanning Tunneling Microscopy and X-Ray Photoelectron Spectroscopy Studies of Graphene Films Prepared by Sonication-Assisted Dispersion. *ACS Nano* **2011**, *5* (8), 6102–6108. https://doi.org/10.1021/nn1009352.

(20) Review of the Universe. Graphene, Production universe-review.ca.

(21) Yi, M.; Shen, Z. A Review on Mechanical Exfoliation for the Scalable Production of Graphene. *J. Mater. Chem. A* **2015**, *3* (22), 11700–11715. https://doi.org/10.1039/C5TA00252D.

(22) Carlsson, J.-O.; Martin, P. M. Chapter 7 - Chemical Vapor Deposition. In *Handbook of Deposition Technologies for Films and Coatings (Third Edition)*; Martin, P. M., Ed.; William Andrew Publishing: Boston, 2010; pp 314–363. https://doi.org/10.1016/B978-0-8155-2031-3.00007-7.

(23) Wassei, J. K.; Mecklenburg, M.; Torres, J. A.; Fowler, J. D.; Regan, B. C.; Kaner, R. B.; Weiller, B. H. Chemical Vapor Deposition of Graphene on Copper from Methane,

Ethane and Propane: Evidence for Bilayer Selectivity. *Small* **2012**, *8* (9), 1415–1422. https://doi.org/10.1002/smll.201102276.

(24) Boyd, D. A.; Lin, W.-H.; Hsu, C.-C.; Teague, M. L.; Chen, C.-C.; Lo, Y.-Y.; Chan, W.-Y.; Su, W.-B.; Cheng, T.-C.; Chang, C.-S.; Wu, C.-I.; Yeh, N.-C. Single-Step Deposition of High-Mobility Graphene at Reduced Temperatures. *Nature Communications* **2015**, *6* (1), 6620. https://doi.org/10.1038/ncomms7620.

(25) Williams, L.; Pirkle, D. R.; Harshbarger, W.; Ebel, T. Plasma Cleaning Method for Removing Residues in a Plasma Process Chamber. US5647953A.

(26) ACS material. CVD Graphene https://www.acsmaterial.com/blog-detail/cvd-graphene.html.

(27) Hummers, W. S.; Offeman, R. E. Preparation of Graphitic Oxide. *J. Am. Chem. Soc.* **1958**, *80* (6), 1339–1339. https://doi.org/10.1021/ja01539a017.

(28) Green, A. A.; Hersam, M. C. Emerging Methods for Producing Monodisperse Graphene Dispersions. *J. Phys. Chem. Lett.* **2010**, *1* (2), 544–549. https://doi.org/10.1021/jz900235f.

(29) Green, A. A.; Hersam, M. C. Solution Phase Production of Graphene with Controlled Thickness via Density Differentiation. *Nano Lett.* **2009**, *9* (12), 4031–4036. https://doi.org/10.1021/nl902200b.

(30) Cheng, M.; Yang, R.; Zhang, L.; Shi, Z.; Yang, W.; Wang, D.; Xie, G.; Shi, D.; Zhang, G. Restoration of Graphene from Graphene Oxide by Defect Repair. *Carbon* **2012**, *50* (7), 2581–2587. https://doi.org/10.1016/j.carbon.2012.02.016.

(31) Park, S.; An, J.; Jung, I.; Piner, R. D.; An, S. J.; Li, X.; Velamakanni, A.; Ruoff, R. S. Colloidal Suspensions of Highly Reduced Graphene Oxide in a Wide Variety of Organic Solvents. *Nano Lett.* **2009**, *9* (4), 1593–1597. https://doi.org/10.1021/nl803798y.

(32) Liu, M.; Zhang, X.; Wu, W.; Liu, T.; Liu, Y.; Guo, B.; Zhang, R. One-Step Chemical Exfoliation of Graphite to ~100% Few-Layer Graphene with High Quality and Large Size at Ambient Temperature. *Chemical Engineering Journal* **2019**, *355*, 181–185. https://doi.org/10.1016/j.cej.2018.08.146.

(33) Yu, P.; Lowe, S. E.; Simon, G. P.; Zhong, Y. L. Electrochemical Exfoliation of Graphite and Production of Functional Graphene. *Current Opinion in Colloid & Interface Science* **2015**, *20* (5), 329–338. https://doi.org/10.1016/j.cocis.2015.10.007.

(34) Zhong, Y. L.; Tian, Z.; Simon, G. P.; Li, D. Scalable Production of Graphene via Wet Chemistry: Progress and Challenges. *Materials Today* **2015**, *18* (2), 73–78. https://doi.org/10.1016/j.mattod.2014.08.019.

(35) Liu, J.; Yang, H.; Zhen, S. G.; Poh, C. K.; Chaurasia, A.; Luo, J.; Wu, X.; Yeow, E. K. L.; Sahoo, N. G.; Lin, J.; Shen, Z. A Green Approach to the Synthesis of High-Quality Graphene Oxide Flakes via Electrochemical Exfoliation of Pencil Core. *RSC Adv.* **2013**, *3* (29), 11745–11750. https://doi.org/10.1039/C3RA41366G.

(36) Abdelkader, A. M.; Kinloch, I. A.; Dryfe, R. A. W. Continuous Electrochemical Exfoliation of Micrometer-Sized Graphene Using Synergistic Ion Intercalations and Organic Solvents. *ACS Appl. Mater. Interfaces* **2014**, *6* (3), 1632–1639. https://doi.org/10.1021/am404497n.

(37) Achee, T. C.; Sun, W.; Hope, J. T.; Quitzau, S. G.; Sweeney, C. B.; Shah, S. A.; Habib, T.; Green, M. J. High-Yield Scalable Graphene Nanosheet Production from Compressed Graphite Using Electrochemical Exfoliation. *Sci Rep* **2018**, *8* (1), 14525. https://doi.org/10.1038/s41598-018-32741-3.

(38) Liu, J.; Poh, C. K.; Zhan, D.; Lai, L.; Lim, S. H.; Wang, L.; Liu, X.; Gopal Sahoo, N.; Li, C.; Shen, Z.; Lin, J. Improved Synthesis of Graphene Flakes from the Multiple Electrochemical Exfoliation of Graphite Rod. *Nano Energy* **2013**, *2* (3), 377–386. https://doi.org/10.1016/j.nanoen.2012.11.003.

(39) Bjerglund, E. T.; Kristensen, M. E. P.; Stambula, S.; Botton, G. A.; Pedersen, S. U.; Daasbjerg, K. Efficient Graphene Production by Combined Bipolar Electrochemical Intercalation and High-Shear Exfoliation. *ACS Omega* **2017**, *2* (10), 6492–6499. https://doi.org/10.1021/acsomega.7b01057.

(40) Hashimoto, H.; Muramatsu, Y.; Nishina, Y.; Asoh, H. Bipolar Anodic Electrochemical Exfoliation of Graphite Powders. *Electrochemistry Communications* **2019**, *104*, 106475. https://doi.org/10.1016/j.elecom.2019.06.001.

(41) Sorensen, C.; Neapl, A.; Singh, G. P. Process for High-Yield Production of Graphene via Detonation of Carbon-Containing Material. US 20140335010 A1.

(42) Seo, D. H.; Pineda, S.; Fang, J.; Gozukara, Y.; Yick, S.; Bendavid, A.; Lam, S. K. H.; Murdock, A. T.; Murphy, A. B.; Han, Z. J.; Ostrikov, K. (Ken). Single-Step Ambient-Air Synthesis of Graphene from Renewable Precursors as Electrochemical Genosensor. *Nature Communications* **2017**, *8* (1), 14217. https://doi.org/10.1038/ncomms14217.

(43) American Elements. Graphite powder https://www.americanelements.com/graphite-powder-7782-42-5.

(44) Sigma-Aldrich. Graphite https://www.sigmaaldrich.com/catalog/product/aldrich/496588?lang=en&region=US.

(45) Keithley. Keithley 2400 Soruce Meter Datasheet.

(46) Parvez, K.; Wu, Z.-S.; Li, R.; Liu, X.; Graf, R.; Feng, X.; Müllen, K. Exfoliation of Graphite into Graphene in Aqueous Solutions of Inorganic Salts. *J. Am. Chem. Soc.* **2014**, *136* (16), 6083–6091. https://doi.org/10.1021/ja5017156.

(47) Abdelkader, A. M.; Cooper, A. J.; Dryfe, R. A. W.; Kinloch, I. A. How to Get between the Sheets: A Review of Recent Works on the Electrochemical Exfoliation of Graphene Materials from Bulk Graphite. *Nanoscale* **2015**, *7* (16), 6944–6956. https://doi.org/10.1039/C4NR06942K.

(48) Nurhafizah, M. D.; Suriani, A. B.; Mohamed, A.; Soga, T. Effect of Voltage Applied for Graphene Oxide/Latex Nanocomposites Produced via Electrochemical Exfoliation and Its Application as Conductive Electrodes. *Diamond and Related Materials* **2020**, *101*, 107624. https://doi.org/10.1016/j.diamond.2019.107624.

(49) Whatman. membrane filters nylon https://www.sigmaaldrich.com/catalog/product/aldrich/wha7402004?lang=en&region=US&cm_sp=Insite-_-caContent_prodMerch_gruCrossEntropy-_-prodMerch10-3.

(50) METTLER TOLEDO. Datasheet Excellence Plus XP Anaytical Balances.

(51) Munz, M.; Giusca, C. E.; Myers-Ward, R. L.; Gaskill, D. K.; Kazakova, O. Thickness-Dependent Hydrophobicity of Epitaxial Graphene. *ACS Nano* **2015**, *9* (8), 8401–8411. https://doi.org/10.1021/acsnano.5b03220.

(52) Tavakoli, F.; Salavati-Niasari, M.; badiei, A.; Mohandes, F. Green Synthesis and Characterization of Graphene Nanosheets. *Materials Research Bulletin* **2015**, *63*, 51–57. https://doi.org/10.1016/j.materresbull.2014.11.045.

(53) Yue, L.; Pircheraghi, G.; Monemian, S. A.; Manas-Zloczower, I. Epoxy Composites with Carbon Nanotubes and Graphene Nanoplatelets – Dispersion and Synergy Effects. *Carbon* **2014**, *78*, 268–278. https://doi.org/10.1016/j.carbon.2014.07.003.

(54) Greinke, R. A.; Reyolds, R. A. Expandable Graphite and Method. Patent US6416815B2.

(55) Mahanandia, P.; Simon, F.; Heinrich, G.; Nanda, K. K. An Electrochemical Method for the Synthesis of Few Layer Graphene Sheets for High Temperature Applications. *Chem. Commun.* **2014**, *50* (35), 4613. https://doi.org/10.1039/c3cc48055k.

(56) Lowe, S. E.; Shi, G.; Zhang, Y.; Qin, J.; Jiang, L.; Jiang, S.; Al-Mamun, M.; Liu, P.; Zhong, Y. L.; Zhao, H. The Role of Electrolyte Acid Concentration in the Electrochemical Exfoliation of Graphite: Mechanism and Synthesis of Electrochemical Graphene Oxide. *Nano Materials Science* **2019**, *1* (3), 215–223. https://doi.org/10.1016/j.nanoms.2019.07.001.

(57) Zangmeister, R. A.; Morris, T. A.; Tarlov, M. J. Characterization of Polydopamine Thin Films Deposited at Short Times by Autoxidation of Dopamine. *Langmuir* **2013**, *29* (27), 8619–8628. https://doi.org/10.1021/la400587j.

(58) Clark, M. B.; Gardella, J. A.; Schultz, T. M.; Patil, D. G.; Salvati, Lawrence. Solid-State Analysis of Eumelanin Biopolymers by Electron Spectroscopy for Chemical Analysis. *Anal. Chem.* **1990**, *62* (9), 949–956. https://doi.org/10.1021/ac00208a011.

(59) Krishnamoorthy, K.; Veerapandian, M.; Yun, K.; Kim, S.-J. The Chemical and Structural Analysis of Graphene Oxide with Different Degrees of Oxidation. *Carbon* **2013**, *53*, 38–49. https://doi.org/10.1016/j.carbon.2012.10.013.

(60) Bay Carbon Inc. SP-1 Graphite Powder Data Sheet. Bay City, Michigan.

(61) Eckmann, A.; Felten, A.; Mishchenko, A.; Britnell, L.; Krupke, R.; Novoselov, K. S.; Casiraghi, C. Probing the Nature of Defects in Graphene by Raman Spectroscopy. *Nano Lett.* **2012**, *12* (8), 3925–3930. https://doi.org/10.1021/nl300901a.

(62) Childres, I.; Jauregui, L.; Park, W.; Caoa, H.; Chena, Y. P. Raman Spectroscopy of Graphene and Related Materials. *New Developments in Photon and Materials Research* **2013**, 403–418.

(63) Ferrari, A. C.; Meyer, J. C.; Scardaci, V.; Casiraghi, C.; Lazzeri, M.; Mauri, F.; Piscanec, S.; Jiang, D.; Novoselov, K. S.; Roth, S.; Geim, A. K. Raman Spectrum of Graphene and Graphene Layers. *Phys. Rev. Lett.* **2006**, *97* (18), 187401. https://doi.org/10.1103/PhysRevLett.97.187401.